Diffractive Lensing of Gravitational Waves as a New Probe of Dark Matter*

Mesut Çalışkan,[α]

[1]*Johns Hopkins University*

BCCP Journal Club – 18 November 2025

[α] **caliskan@jhu.edu**

* arXiv: **2201.04619, 2206.02803, 2307.06990**

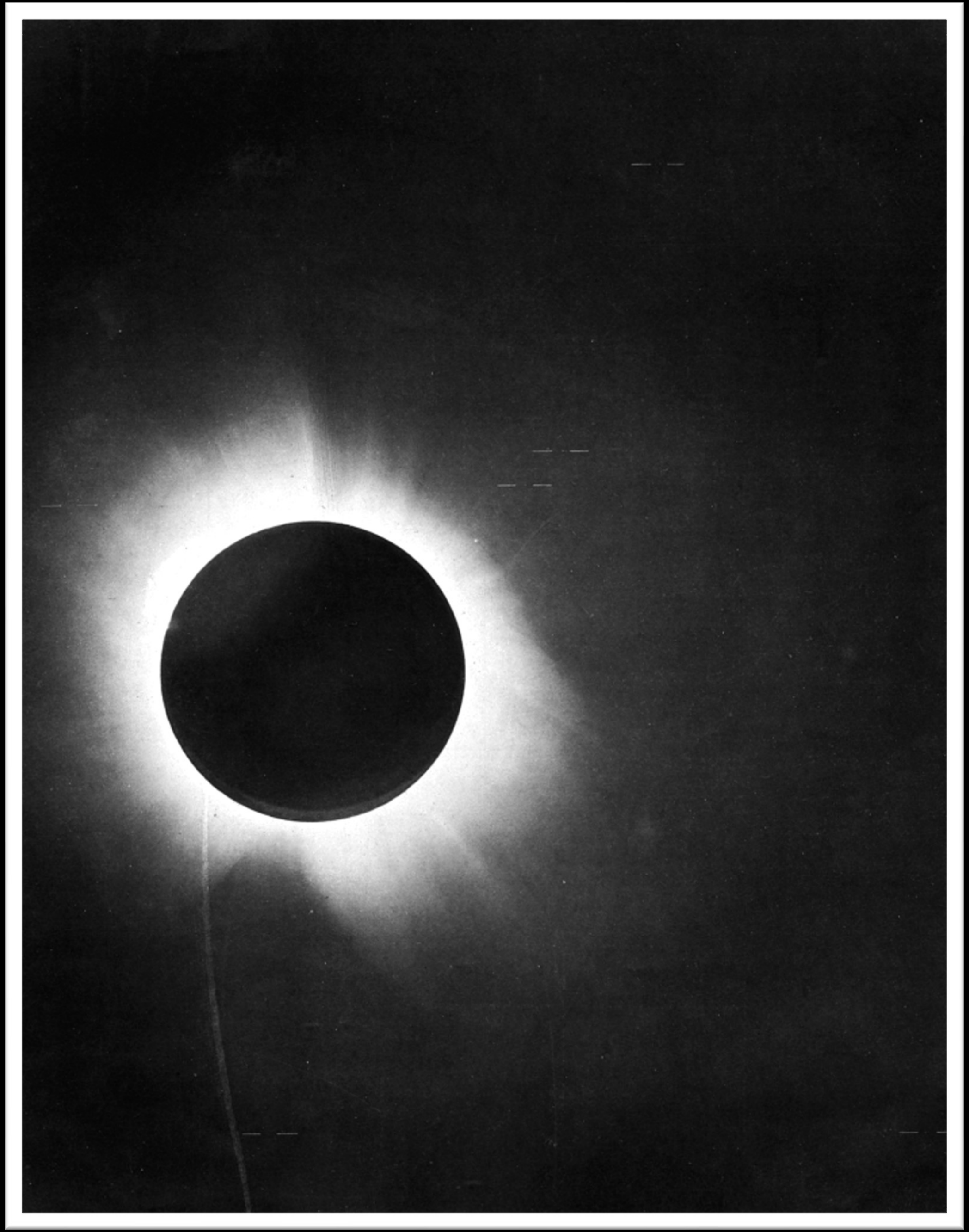

F. W. Dyson, A. S. Eddington, and C. Davidson (1920)

Current techniques are limited to probing dark-matter structures heavier than $\sim 10^8\ M_\odot$.

Current techniques are limited to probing dark-matter structures heavier than $\sim 10^8 \ M_\odot$.

Probing the substructures within DM halos remains challenging because of their faint luminosity and low masses, which lead to much lower detection probabilities.

Current techniques are limited to probing dark-matter structures heavier than $\sim 10^8\ M_\odot$.

Probing the substructures within DM halos remains challenging because of their faint luminosity and low masses, which lead to much lower detection probabilities.

Current techniques are limited to probing dark-matter structures heavier than $\sim 10^8\ M_\odot$.

Probing the substructures within DM halos remains challenging because of their faint luminosity and

low masses , which lead to much lower detection probabilities.

Testbed for the Nature of Dark Matter

Dark Matter

Gravitational Waves

Mass

Profile

Number Density

Strong Lensing of GWs

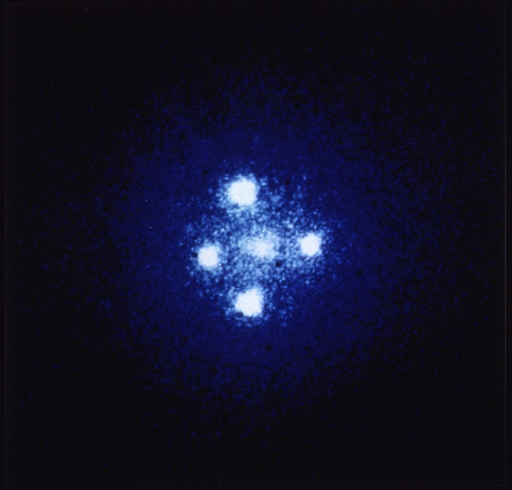

Credit: NASA, ESA, and STScI

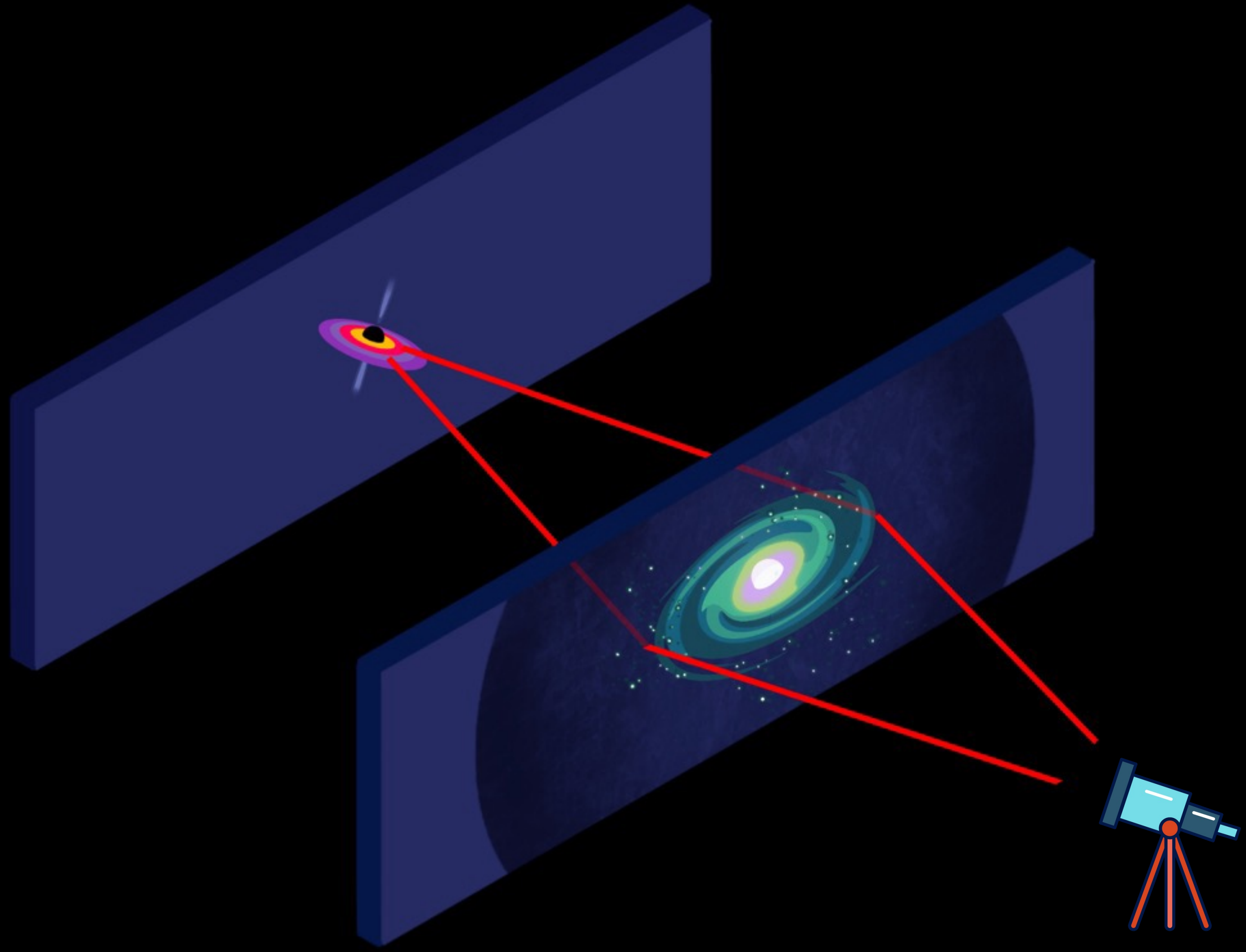

Illustration by Neha Anil Kumar

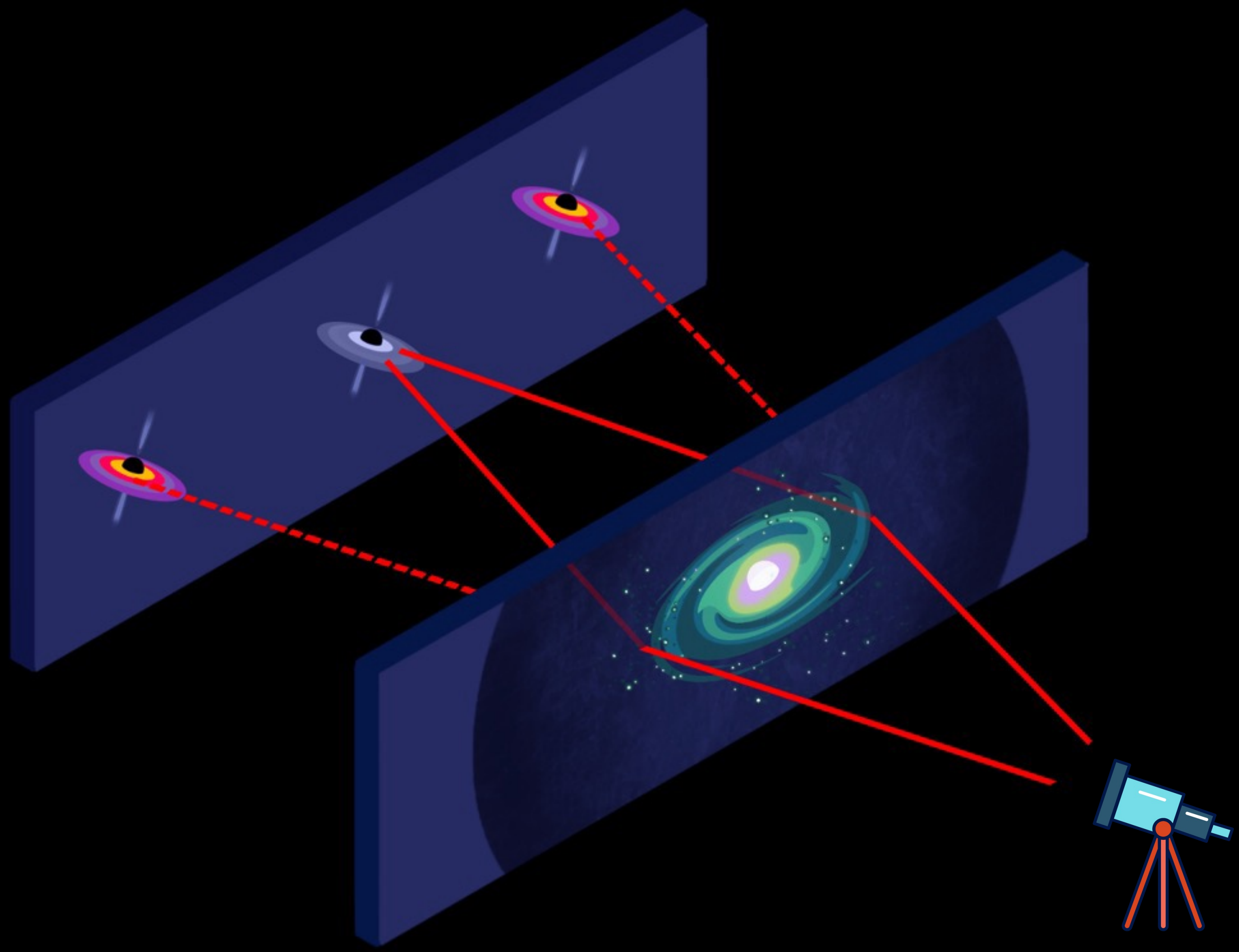

Illustration by Neha Anil Kumar

What if the source is a (massive) binary black hole?

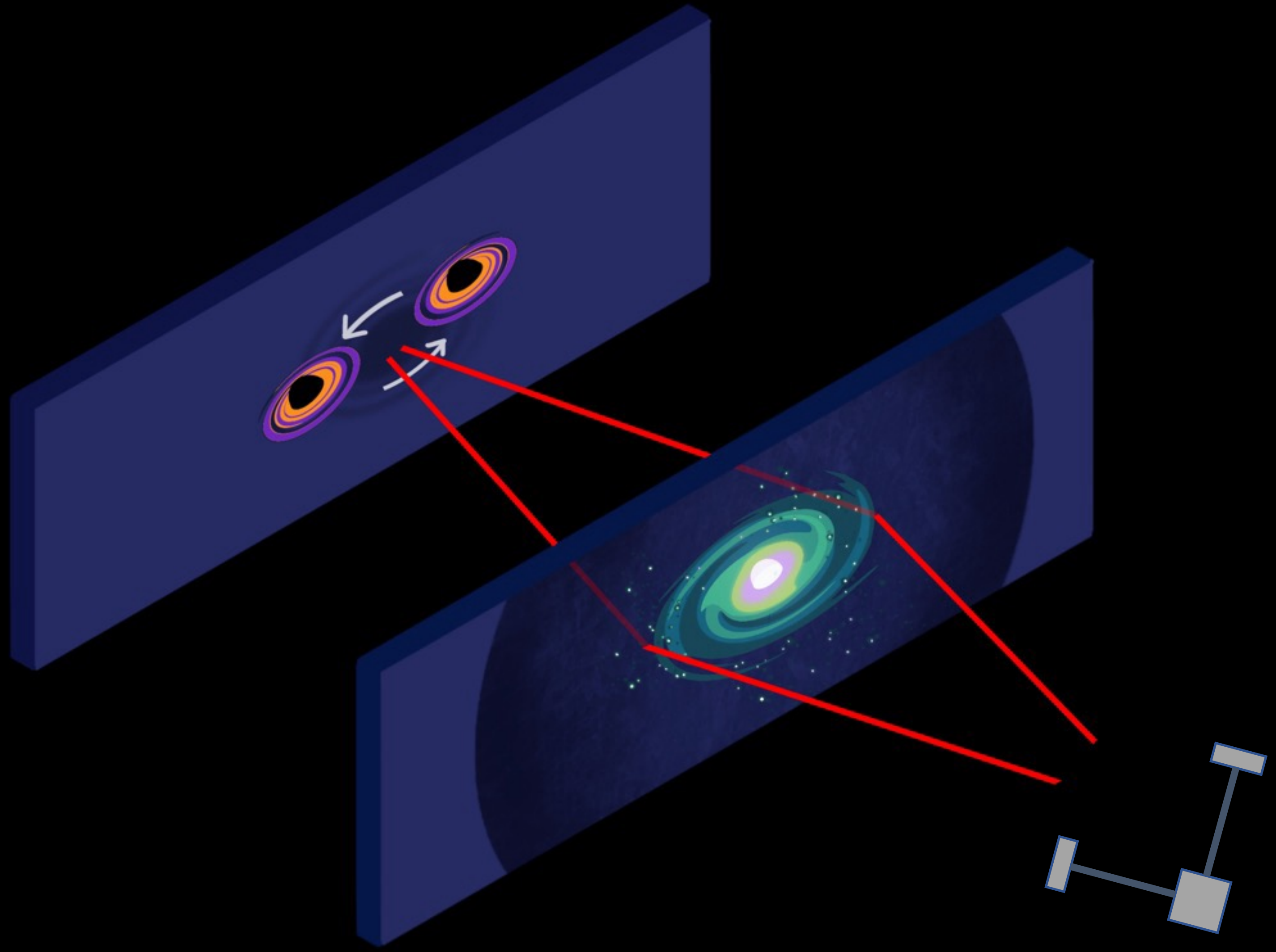

Illustration by Neha Anil Kumar

Unlensed Waveform

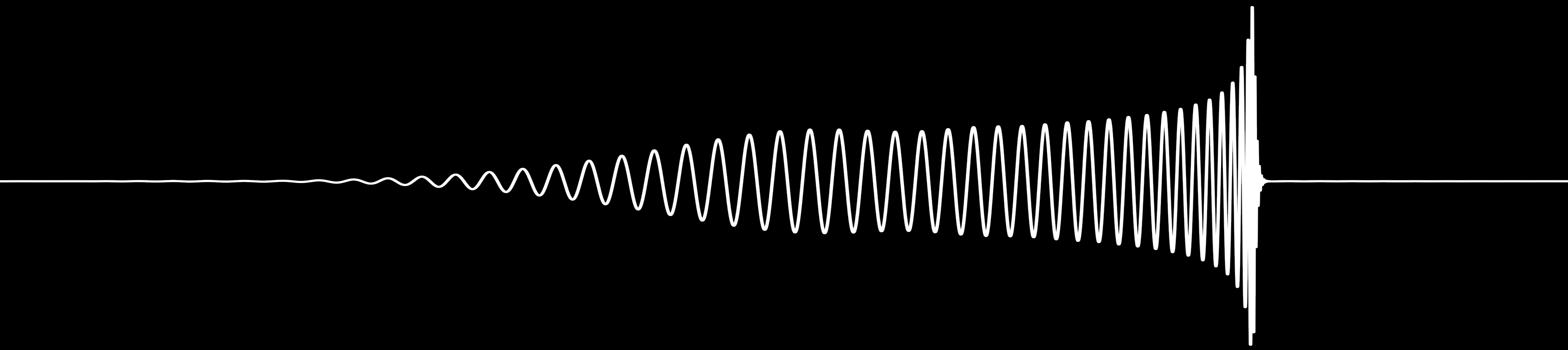

Strongly Lensed Waveforms

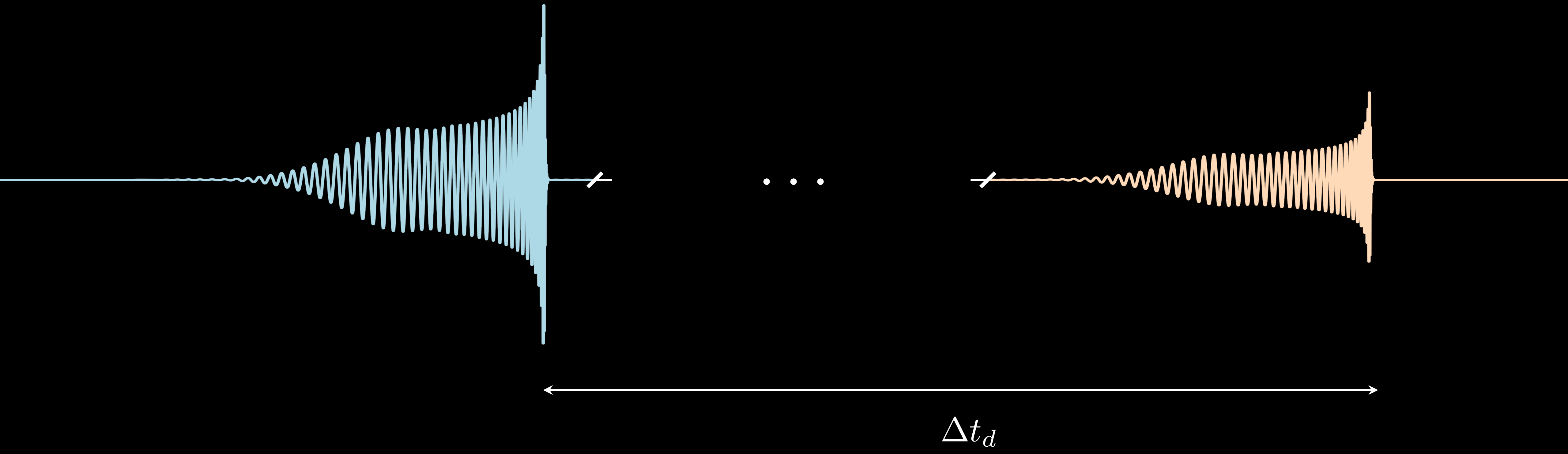

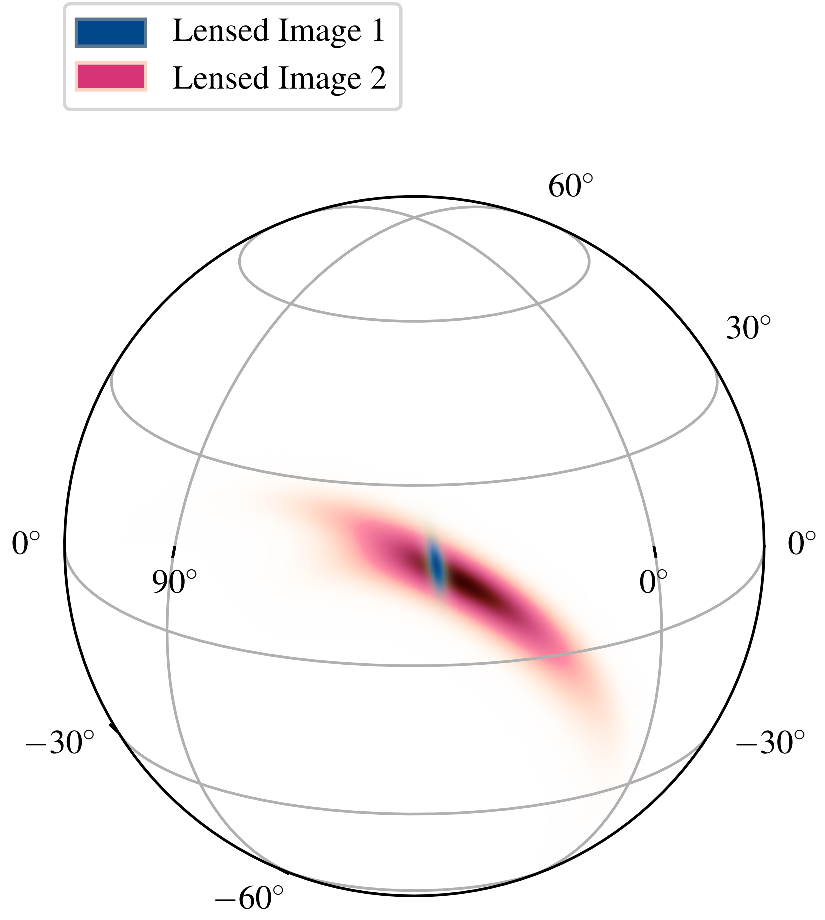

(a) lensed

[2] **Çalışkan** et al. (2022)

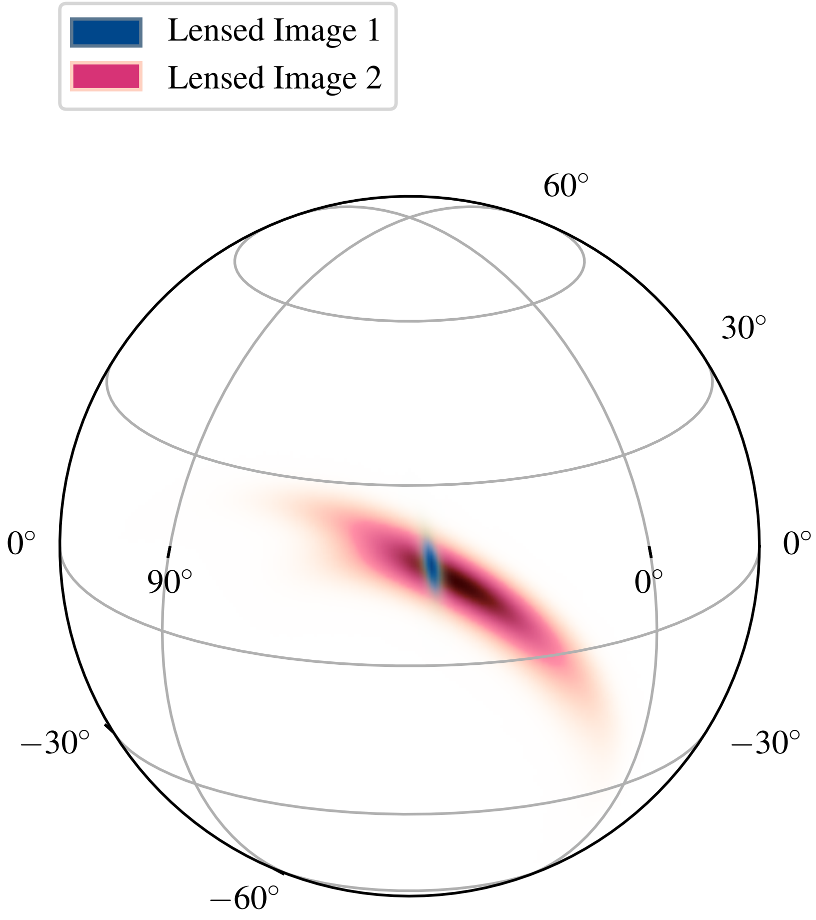

(a) lensed

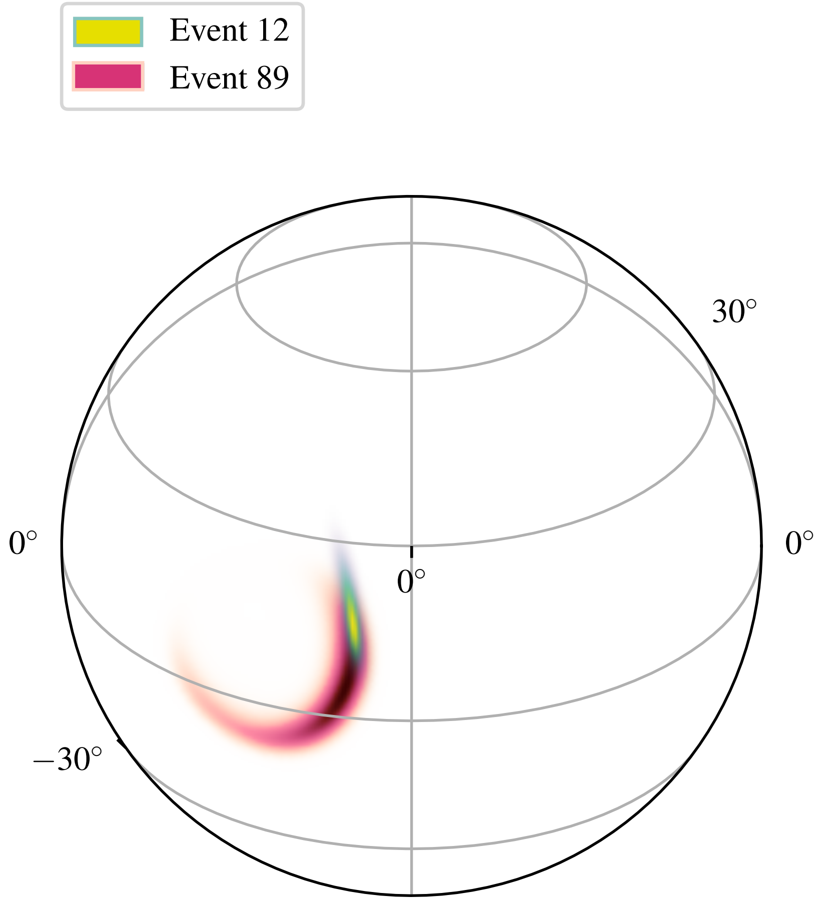

(b) not lensed

[2] **Çalışkan** et al. (2022)

False Alarm Probability

$$\sim \frac{1}{10^4}$$

Strong Lensing Rate?

$$\sim \frac{1}{10^3}$$

Li et al. (2018)

$$N_{\mathrm{lensed}} \propto N_{\mathrm{events}}$$

$$N_{\text{lensed}} \propto N_{\text{events}}$$
$$N_{\text{false alarms}} \propto N_{\text{events}}^2$$

[2] **Çalışkan** et al. (2022)

What if the lens is smaller?

Wave-Optics Effects

$$M_L \lesssim 10^5 \, M_\odot \left(\frac{f}{\mathrm{Hz}} \right)^{-1}$$

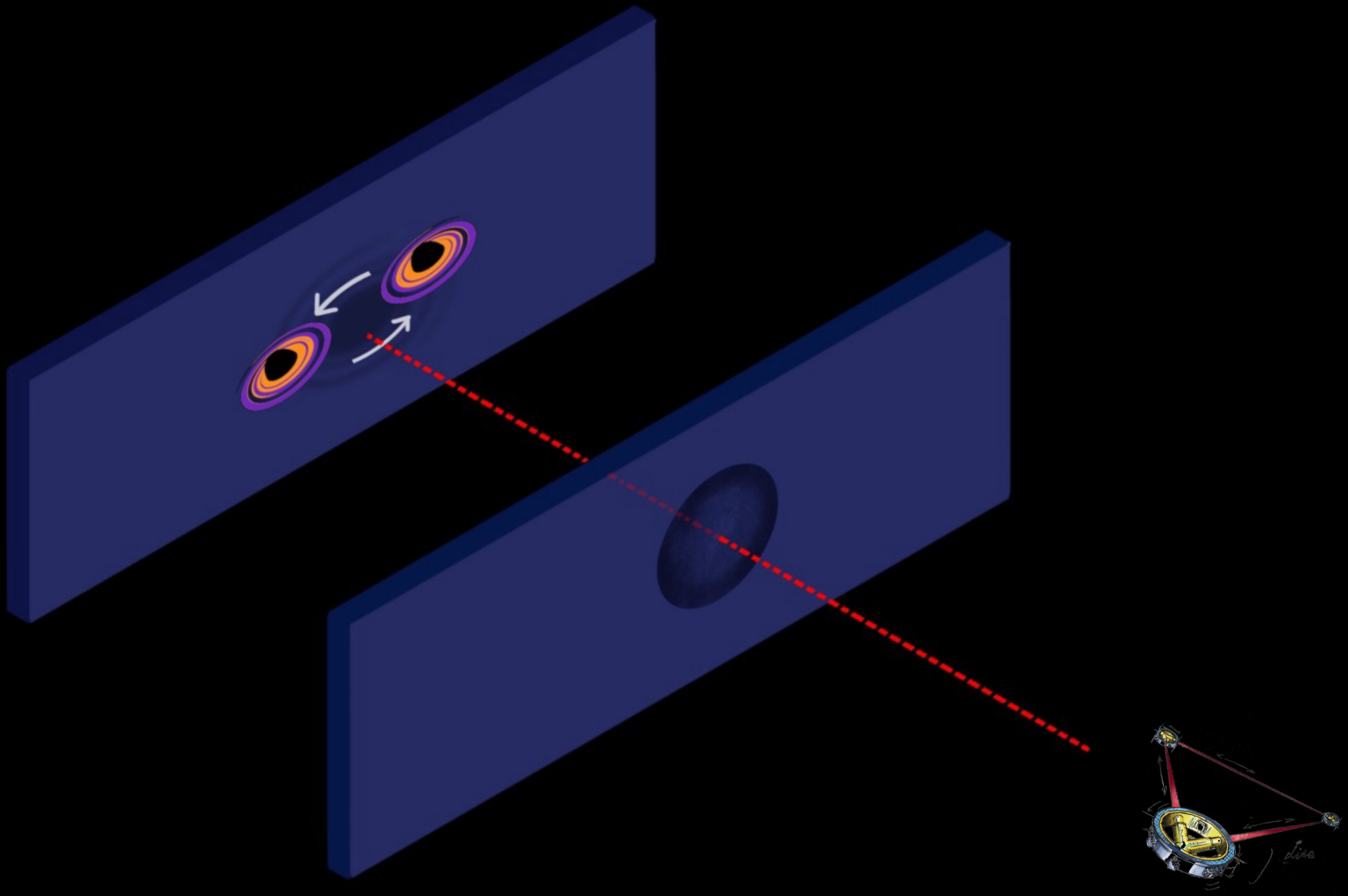

Illustration by Neha Anil Kumar

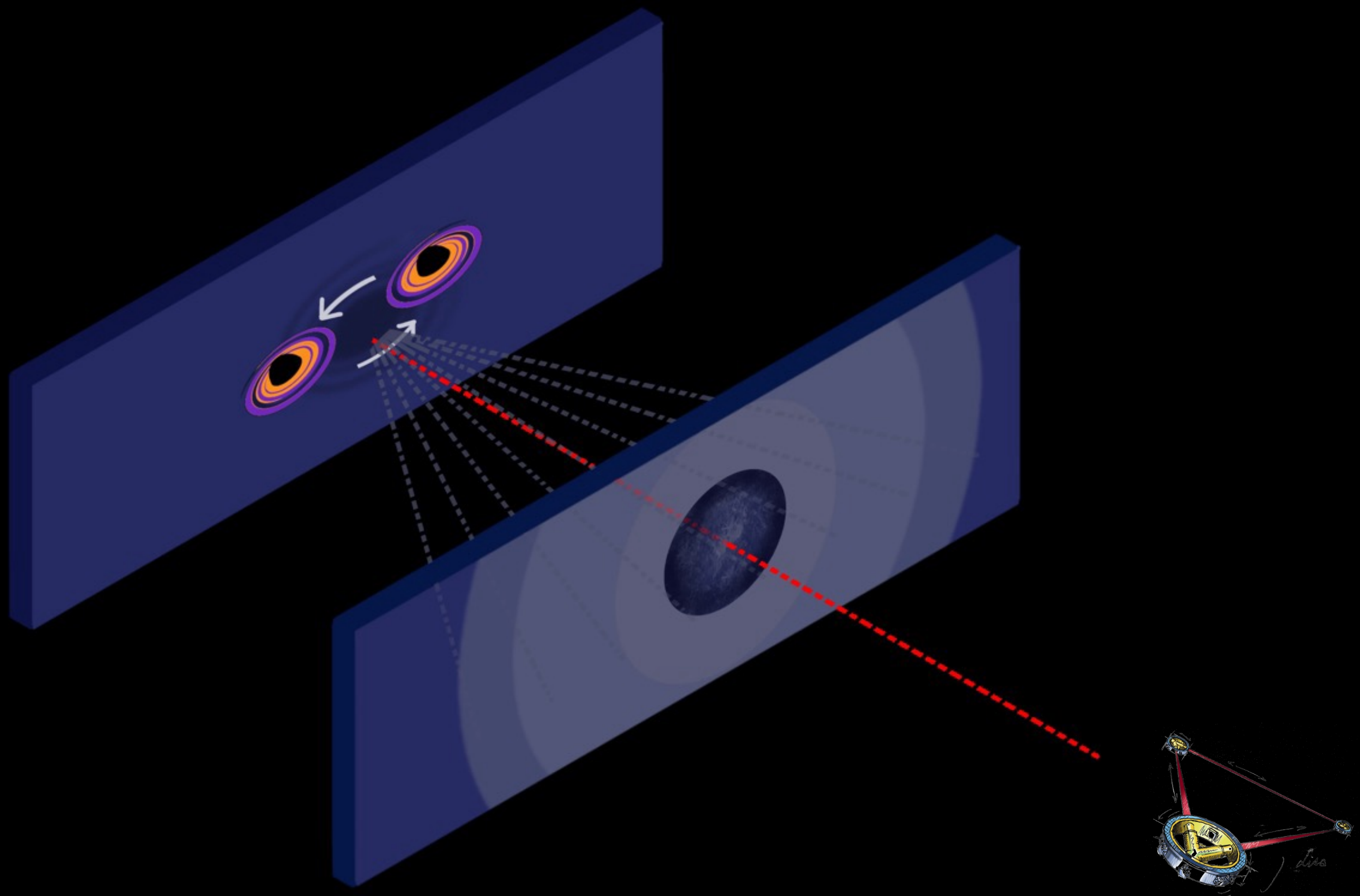

Illustration by Neha Anil Kumar

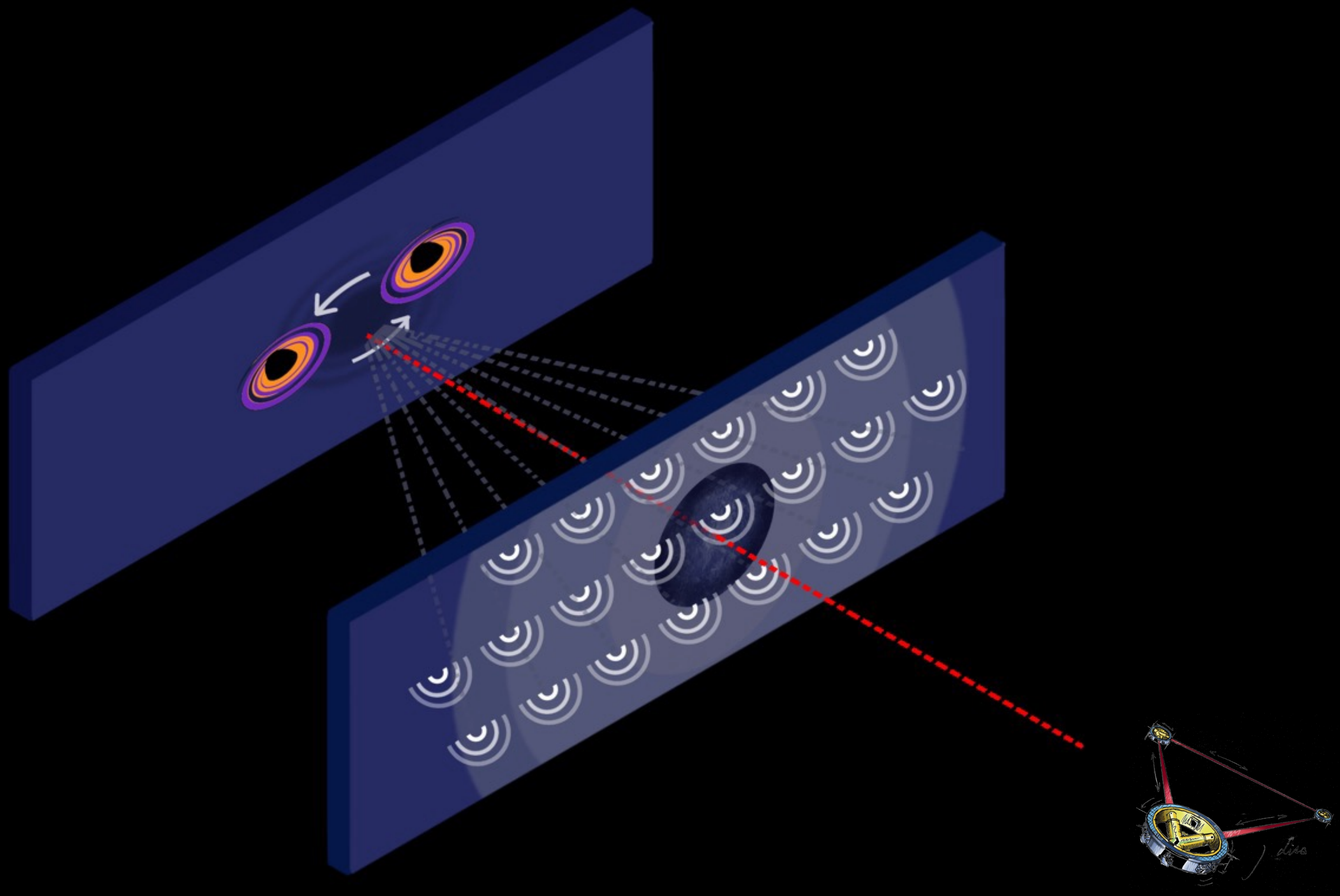

Illustration by Neha Anil Kumar

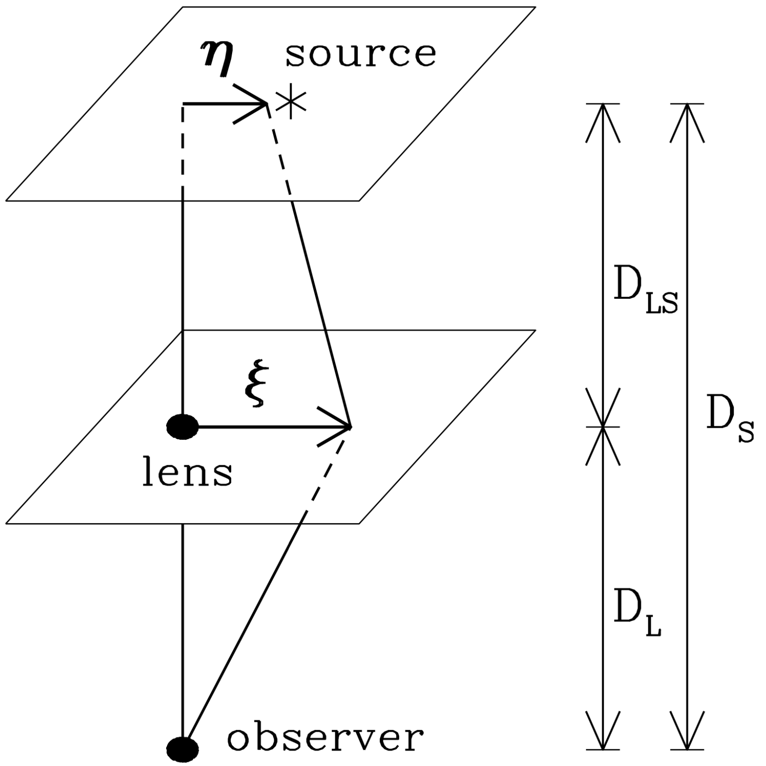

$$\boldsymbol{x} \equiv \frac{\boldsymbol{\xi}}{\xi_0} \quad \text{and} \quad \boldsymbol{y} \equiv \boldsymbol{\eta}\frac{D_{\mathrm{L}}}{\xi_0 D_{\mathrm{S}}}$$

Impact Parameter

Einstein Radius

- $$F(f, \boldsymbol{y}) = \frac{D_{\mathrm{S}}(1+z_{\mathrm{L}})\xi_0^2}{D_{\mathrm{L}}D_{\mathrm{LS}}}\frac{f}{i}\int \mathrm{d}^2\boldsymbol{x}\, \exp[2\pi i f t_{\mathrm{d}}(\boldsymbol{x}, \boldsymbol{y})]$$
- $$t_{\mathrm{d}}(\boldsymbol{x}, \boldsymbol{y}) = \frac{D_{\mathrm{S}}\xi_0^2}{D_{\mathrm{L}}D_{\mathrm{LS}}}(1+z_{\mathrm{L}})\left[\frac{1}{2}|\boldsymbol{x}-\boldsymbol{y}|^2 - \psi(\boldsymbol{x}) + \phi(\boldsymbol{y})\right]$$
- $$w = 8\pi M_{\mathrm{Lz}} f$$

Deflection Potential

(Based on the Matter Distribution of the Lens)

Lensed Waveform in the Frequency Domain: $\tilde{h}^L(f; w, y) = F(w, y)\tilde{h}(f)$

Geometrical optics limit: frequency-independent magnification, time delay, and phase shift

Wave optics effects: frequency-dependent modulations in the amplitude and phase of the waveform (directly dependent on the profile and mass of the lens)

[1] Takahashi and Nakamura (2003)

Lensing of Gravitational Waves

- The wavelength of GWs can be comparable to the size of the lenses, leading to ***frequency-dependent* modulations in the waveform phase and amplitude** due to wave-optics (WO) effects.

- This allows for the possibility of **infer the lens properties** from a single GW observation.

- WO effects can lead to **lensing detectability with cross sections larger than those achievable with the observation of multiple "images."**

[1] Takahashi and Nakamura (2003)
[3] **Çalışkan** et al. (2023a)
[4] **Çalışkan**, et al. (2023b)
[5] Tambalo et al. (2022)
[6] Fairbairn et al. (2022)
[7] Savastano et al. (2023)
[8] Ji and Dai (2024)
[9] Leung et al. (2023)
[10] Dai et al. (2018)

Also:
[11] Feldbrugge, Pen, and Turok (2023)
[12] Feldbrugge and Turok (2020)
[13] Jow and Pen (2022)
[11] Jow and Pen (2024)
[12] Villarrubia-Rojo et al. (2024)

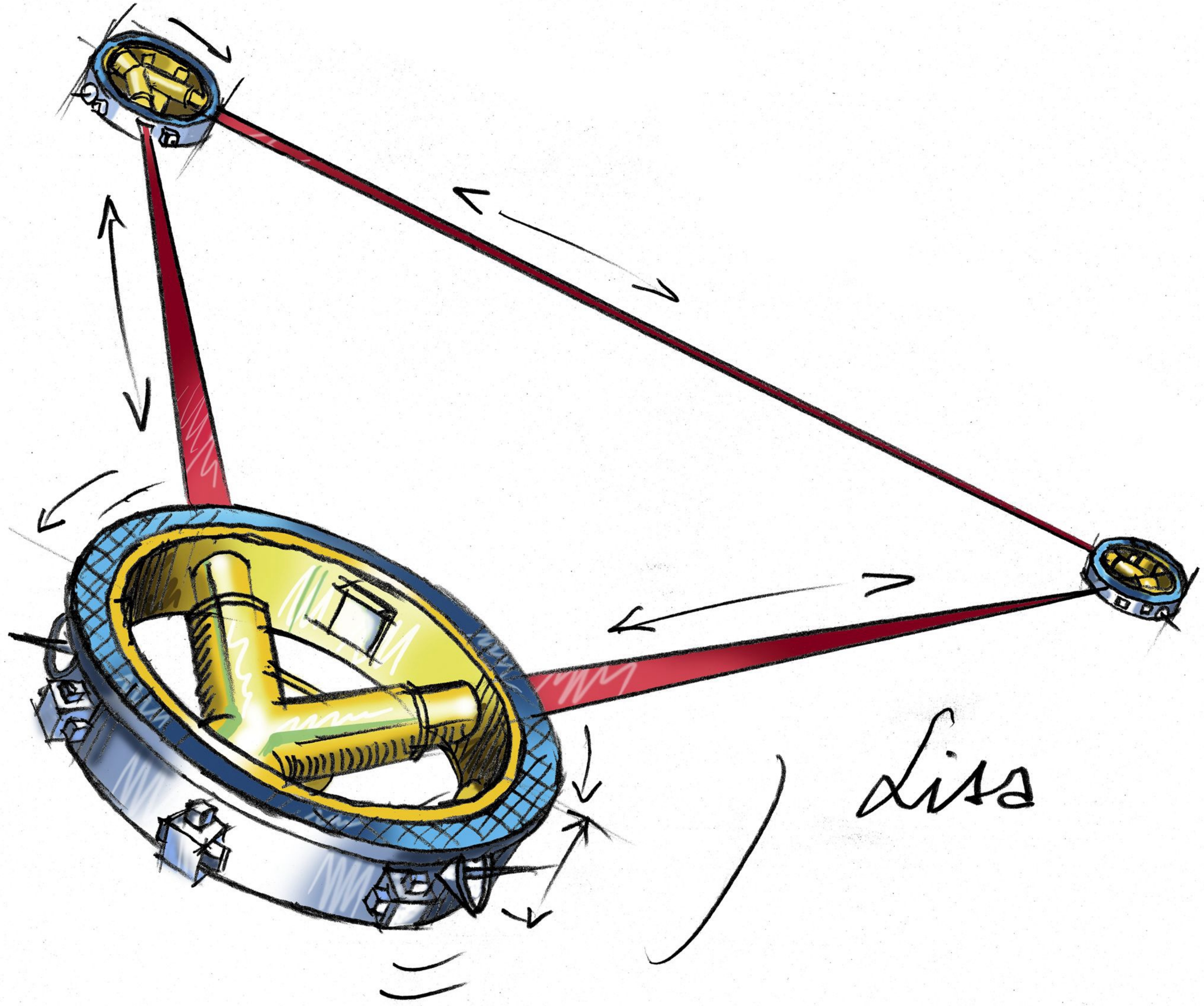

[Credit:] ESA - C. Vijoux

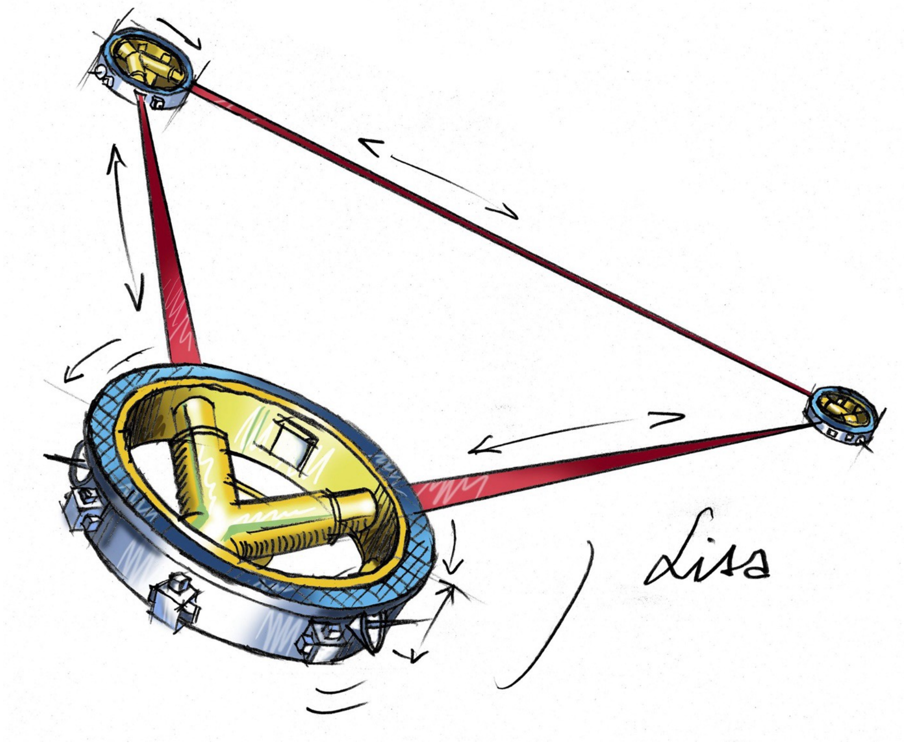

Laser Interferometer Space Antenna (LISA)

- LISA will be the first dedicated space-based gravitational-wave observatory.
- LISA will detect gravitational waves (GWs) emitted by massive black hole binaries (MBHBs) in the low-frequency (~mHz) band.
- These MBHBs ($M_{\mathrm{Total}} \approx 10^4 - 10^8\, M_{\odot}$) will have high SNRs and large redshifts.
- Low-mass lenses, such as dark-matter (DM) subhalos, have sizes comparable to the wavelength of these GWs.

As such, MBHBs are excellent candidates for observing WO effects.

[Credit:] ESA-C. Vijoux

Lensed and Unlensed Waveforms

Lensed and Unlensed Waveforms

$$\tilde{h}^L(f; w, y) = F(w, y)\tilde{h}(f)$$

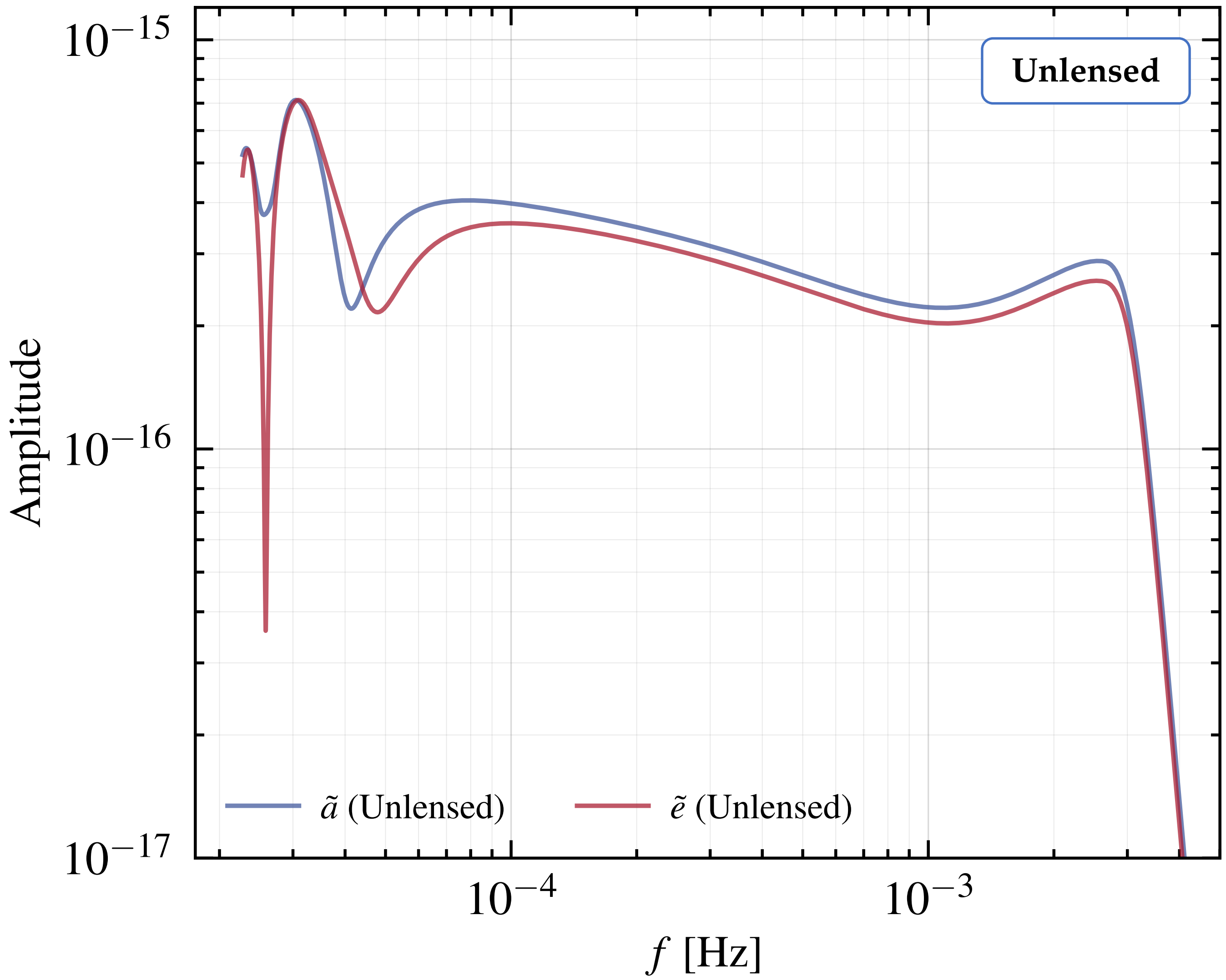

[3] **Çalışkan** et al. (2023a)

Lensed and Unlensed Waveforms

$$\tilde{h}^L(f; w, y) = F(w, y)\tilde{h}(f)$$

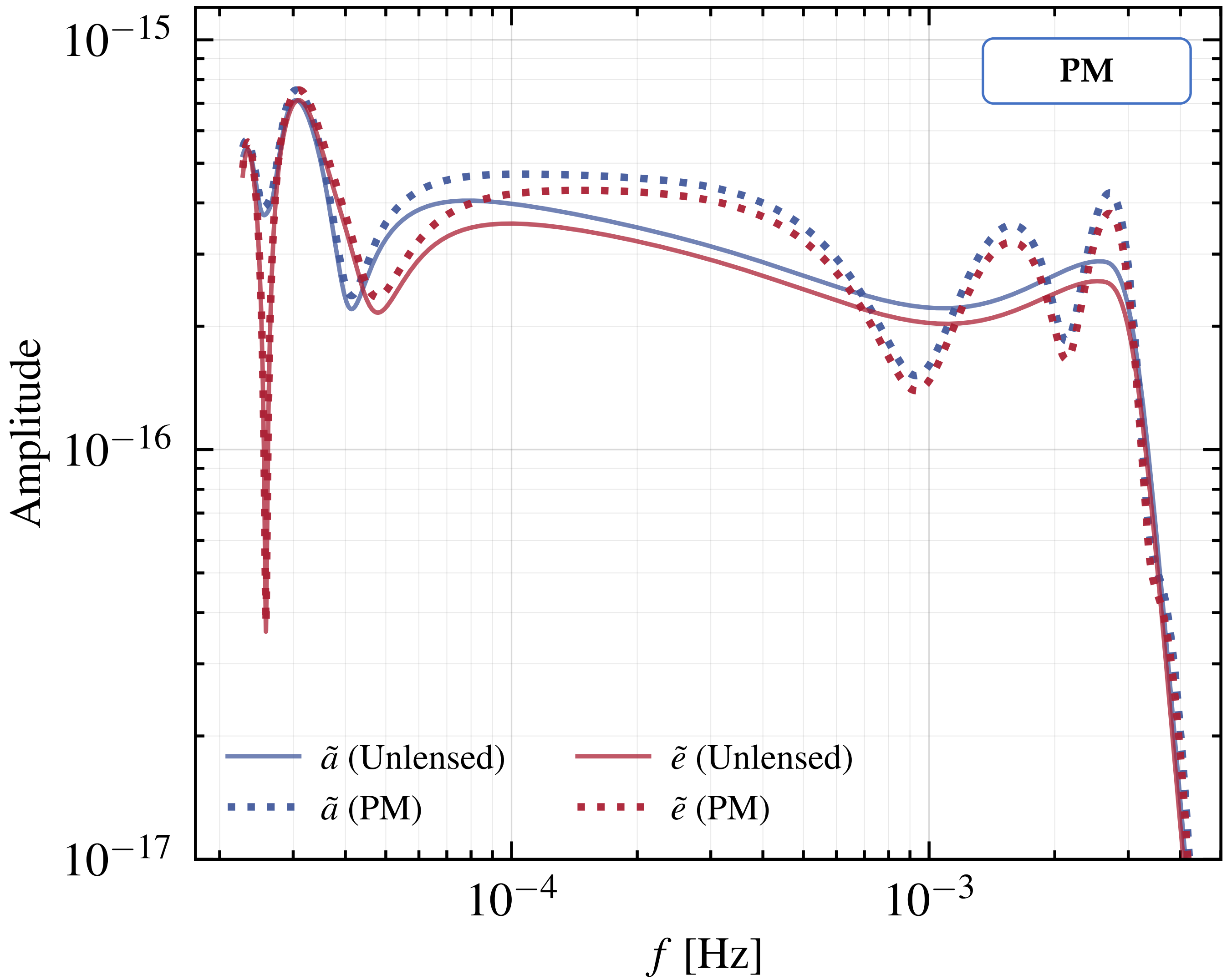

[3] **Çalışkan** et al. (2023a)

Lensed and Unlensed Waveforms

$$\tilde{h}^L(f; w, y) = F(w, y)\tilde{h}(f)$$

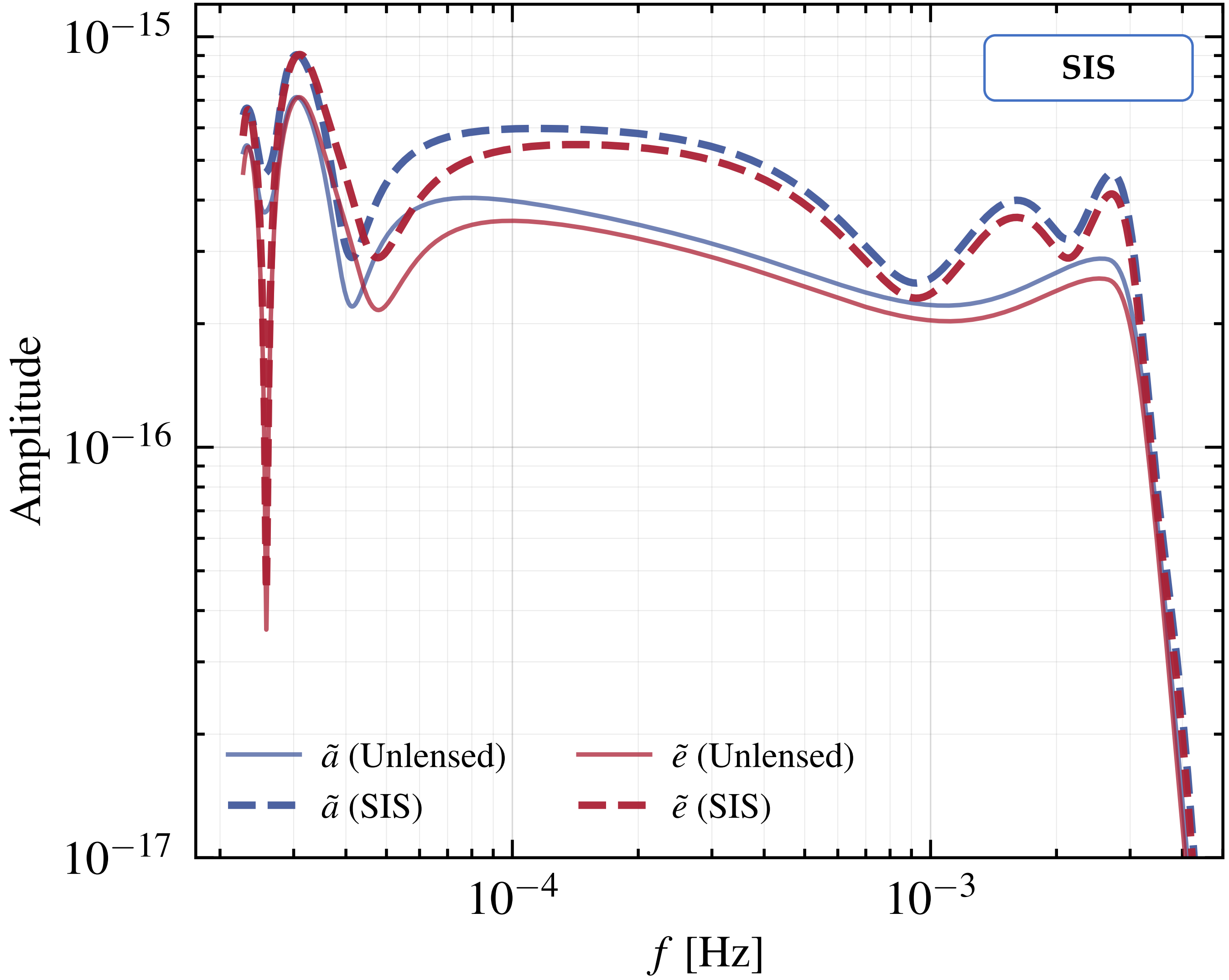

[3] **Çalışkan** et al. (2023a)

Lensed and Unlensed Waveforms

$$\tilde{h}^L(f; w, y) = F(w, y)\tilde{h}(f)$$

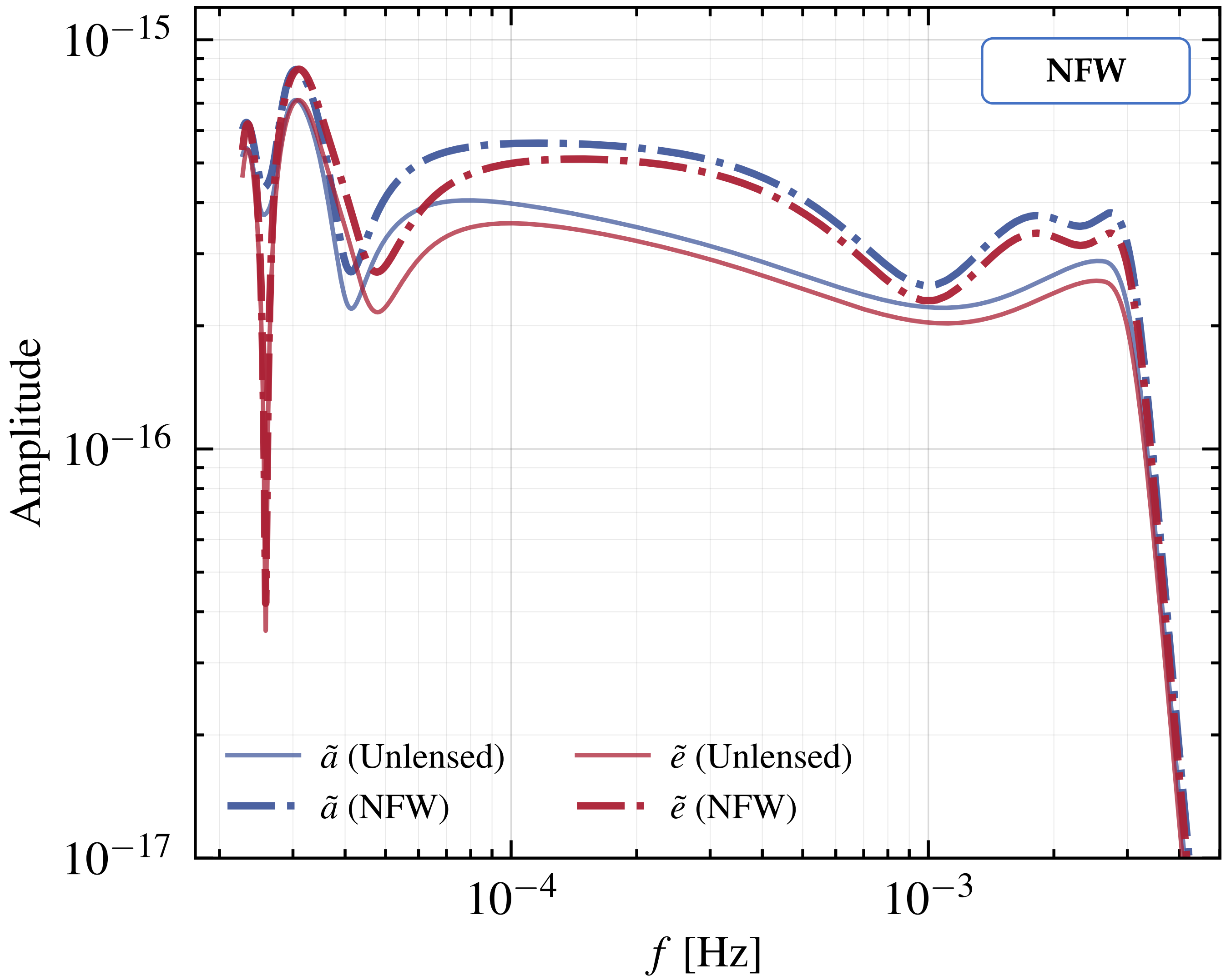

[3] **Çalışkan** et al. (2023a)

Measurability of the Lens Parameters

Measurability of Lens Mass ($M_{\rm Lz}$)

Measurability of Alignment (y)

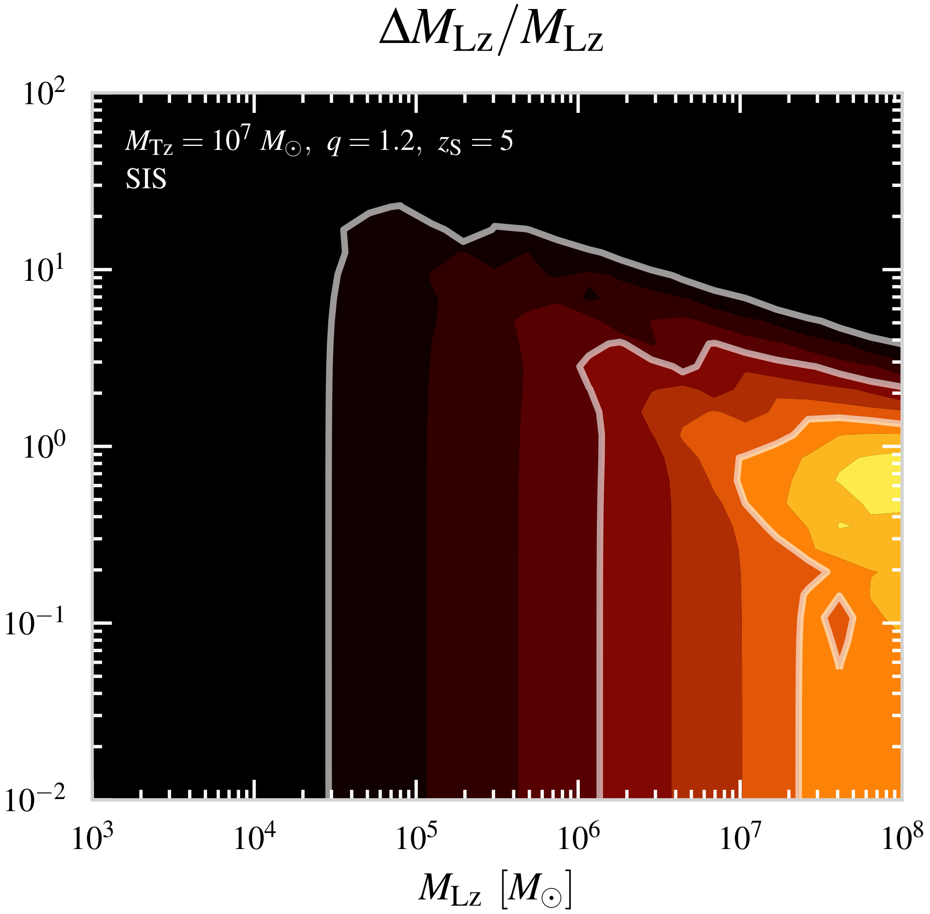

Varying Alignments

Varying Dark Matter Halo (Lens) Masses

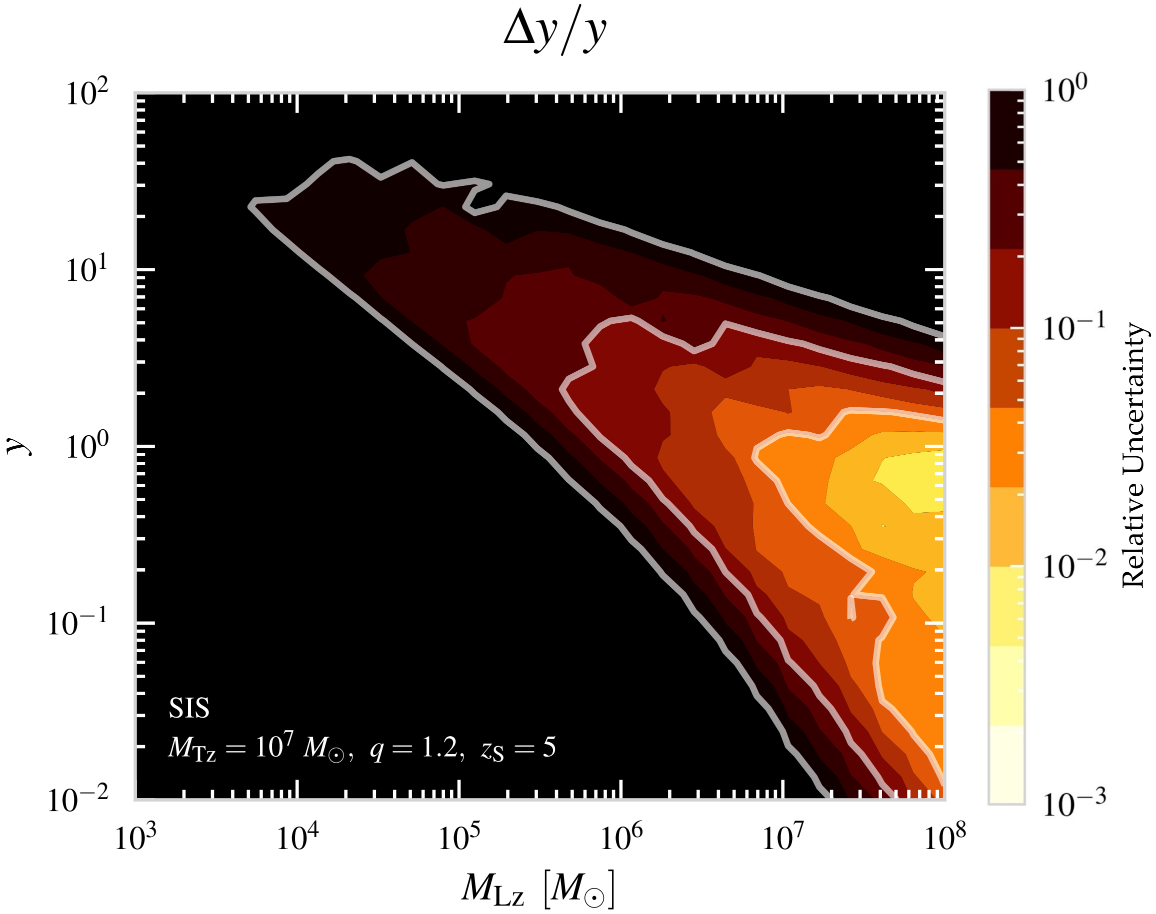

[3] **Çalışkan**, et al. (2023a)
[4] **Çalışkan**, et al. (2023b)

Optical Depth and Probability

Set of Source Parameters

Halo Virial Mass

$$\tau(\boldsymbol{\theta}^{\mathrm{S}} = \{z_{\mathrm{S}}, \dots\}) = \int_0^{z_{\mathrm{S}}} \mathrm{d}z_{\mathrm{L}} \int_{M_{\mathrm{L}}^{\min}}^{M_{\mathrm{L}}^{\max}} \mathrm{d}M_{\mathrm{L}} \, \frac{4\pi M_{\mathrm{L}} D_{\mathrm{LS}}}{D_{\mathrm{L}} D_{\mathrm{S}}} \, y_{\mathrm{cr}}^2(M_{\mathrm{L}}|\boldsymbol{\theta}^{\mathrm{S}}) \, n\left[M_{200}, z_{\mathrm{L}}, z_{\mathrm{S}}\right] \, \chi^2(z_{\mathrm{L}}) \frac{\mathrm{d}\chi(z_{\mathrm{L}})}{\mathrm{d}z_{\mathrm{L}}} \frac{\mathrm{d}M_{200}}{\mathrm{d}M_{\mathrm{L}}}$$

Source Redshift

Lens Redshift

Lens Mass

Critical Impact Parameter

Comoving Number Density of Halos

Comoving Distance

$$P = 1 - e^{-\tau(\boldsymbol{\theta}^{\mathrm{S}} = \{z_{\mathrm{S}}, \dots\})}$$

[4] **Çalışkan,** et al. (2023b)
[2] Schneider et al. (1992)

Optical Depth and Probability

Set of Source Parameters

Halo Virial Mass

$$\tau(\boldsymbol{\theta}^{\mathrm{S}} = \{z_{\mathrm{S}}, \dots\}) = \int_0^{z_{\mathrm{S}}} \mathrm{d}z_{\mathrm{L}} \int_{M_{\mathrm{L}}^{\min}}^{M_{\mathrm{L}}^{\max}} \mathrm{d}M_{\mathrm{L}} \, \frac{4\pi M_{\mathrm{L}} D_{\mathrm{LS}}}{D_{\mathrm{L}} D_{\mathrm{S}}} \, y_{\mathrm{cr}}^2(M_{\mathrm{L}}|\boldsymbol{\theta}^{\mathrm{S}}) \, n\left[M_{200}, z_{\mathrm{L}}, z_{\mathrm{S}}\right] \chi^2(z_{\mathrm{L}}) \frac{\mathrm{d}\chi(z_{\mathrm{L}})}{\mathrm{d}z_{\mathrm{L}}} \frac{\mathrm{d}M_{200}}{\mathrm{d}M_{\mathrm{L}}}$$

Source Redshift

Lens Redshift

Lens Mass

Critical Impact Parameter

Comoving Number Density of Halos

Comoving Distance

[4] **Çalışkan**, et al. (2023b)
[2] Schneider et al. (1992)

Optical Depth and Probability

Set of Source Parameters

Halo Virial Mass

$$\tau(\boldsymbol{\theta}^{\mathrm{S}} = \{z_{\mathrm{S}}, \dots\}) = \int_0^{z_{\mathrm{S}}} \mathrm{d}z_{\mathrm{L}} \int_{M_{\mathrm{L}}^{\mathrm{min}}}^{M_{\mathrm{L}}^{\mathrm{max}}} \mathrm{d}M_{\mathrm{L}}\, \frac{4\pi M_{\mathrm{L}} D_{\mathrm{LS}}}{D_{\mathrm{L}} D_{\mathrm{S}}} \left(y_{\mathrm{cr}}^2 (M_{\mathrm{L}} | \boldsymbol{\theta}^{\mathrm{S}}) \right) n \left[M_{200}, z_{\mathrm{L}}, z_{\mathrm{S}} \right] \chi^2(z_{\mathrm{L}}) \frac{\mathrm{d}\chi(z_{\mathrm{L}})}{\mathrm{d}z_{\mathrm{L}}} \frac{\mathrm{d}M_{200}}{\mathrm{d}M_{\mathrm{L}}}$$

Source Redshift

Lens Redshift

Lens Mass

Critical Impact Parameter

Comoving Number Density of Halos

Comoving Distance

Strong Lensing: $y_{\mathrm{cr}}^{\mathrm{SL}} = 1$

Wave-Optics: $y_{\mathrm{cr}}^{\mathrm{WO}} \in [10, 100]$

[4] **Çalışkan**, et al. (2023b)
[2] Schneider et al. (1992)

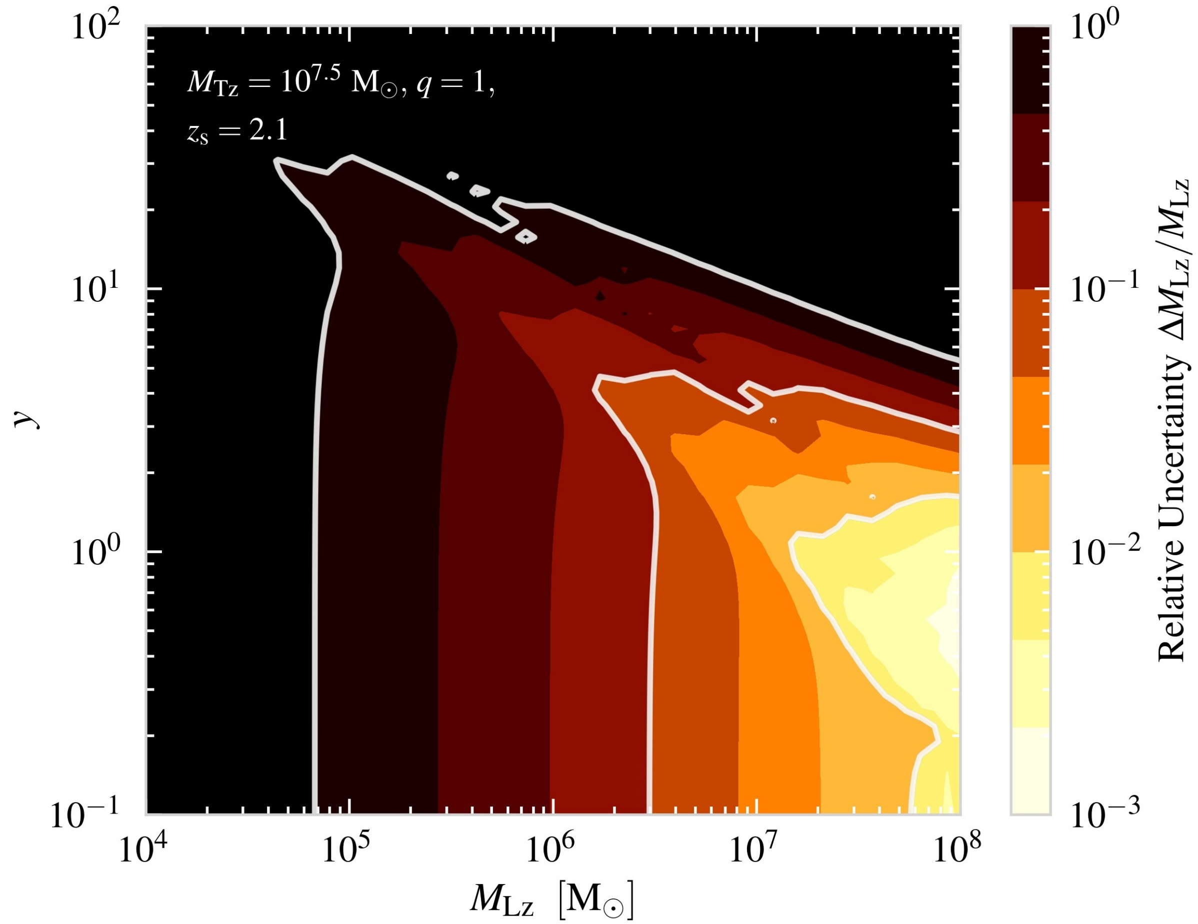

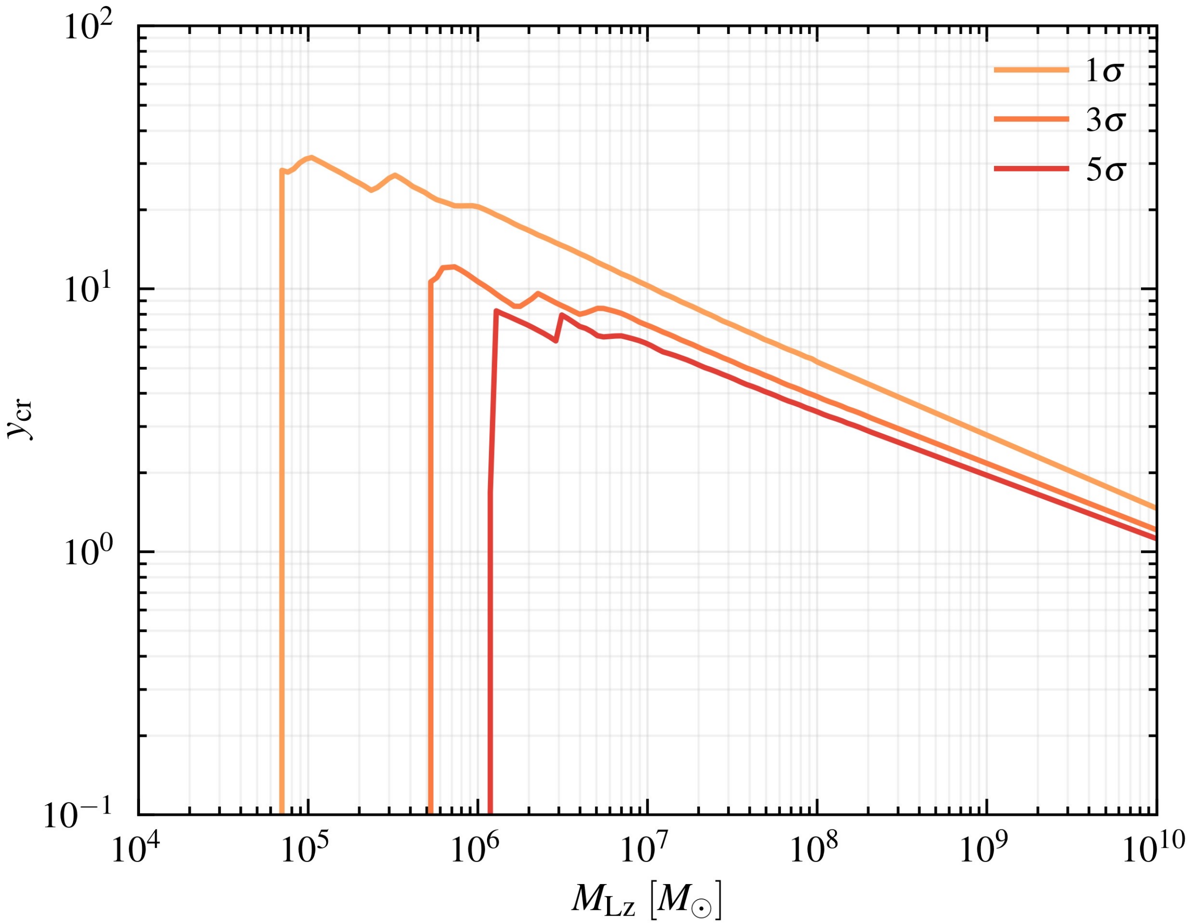

[3] **Çalışkan**, et al. (2023a)
[4] **Çalışkan**, et al. (2023b)

Differential Optical Depth (Probability)

Differential Probability

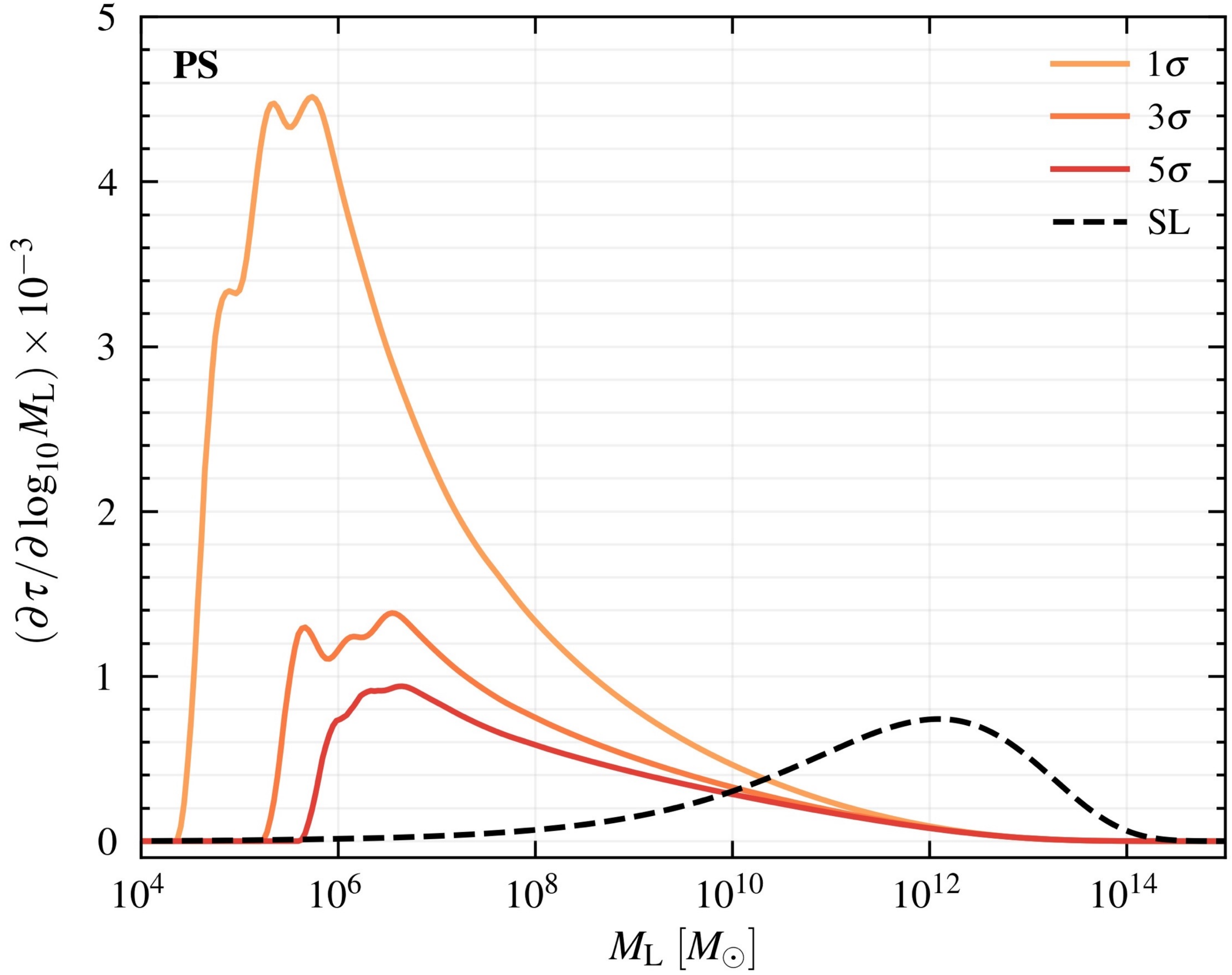

Lens Mass

[3] **Çalışkan**, et al. (2023a)
[4] **Çalışkan**, et al. (2023b)

Detection Probability (Source Model Agnostic)

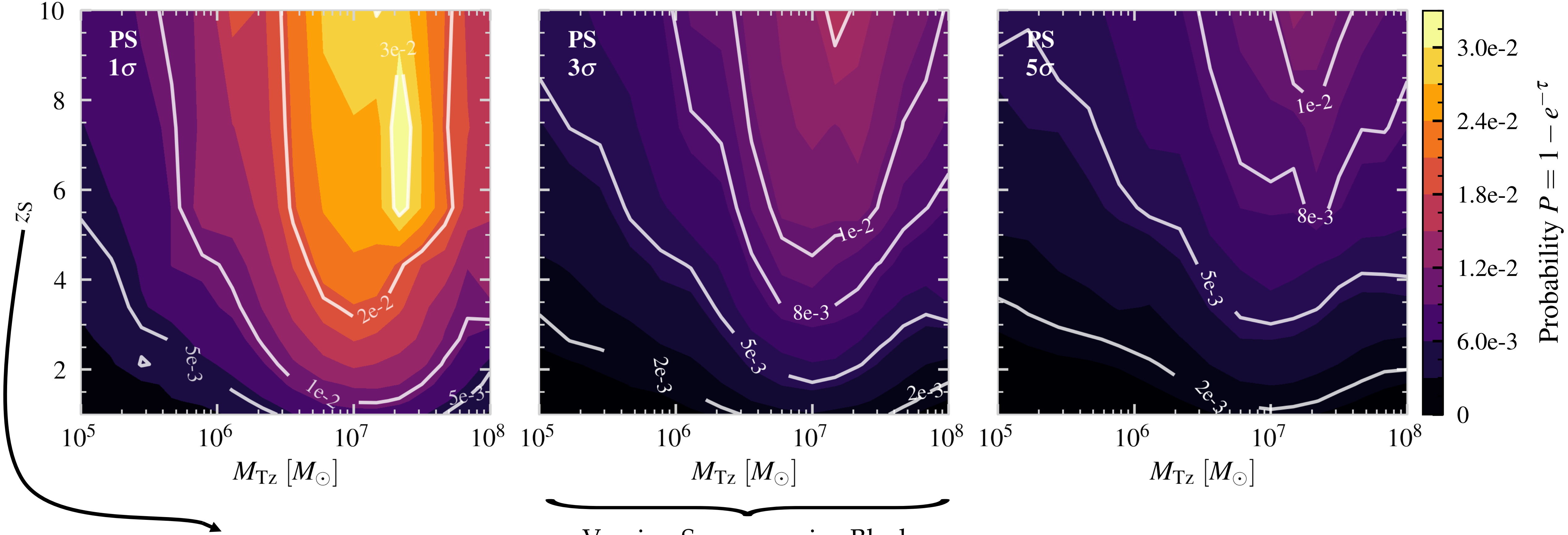

Varying Supermassive Black Hole Masses

Redshift of Supermassive Black Holes (Measure of Distance)

[4] **Çalışkan**, et al. (2023b)

Red MBHBs Are Below Individual Detection Threshold

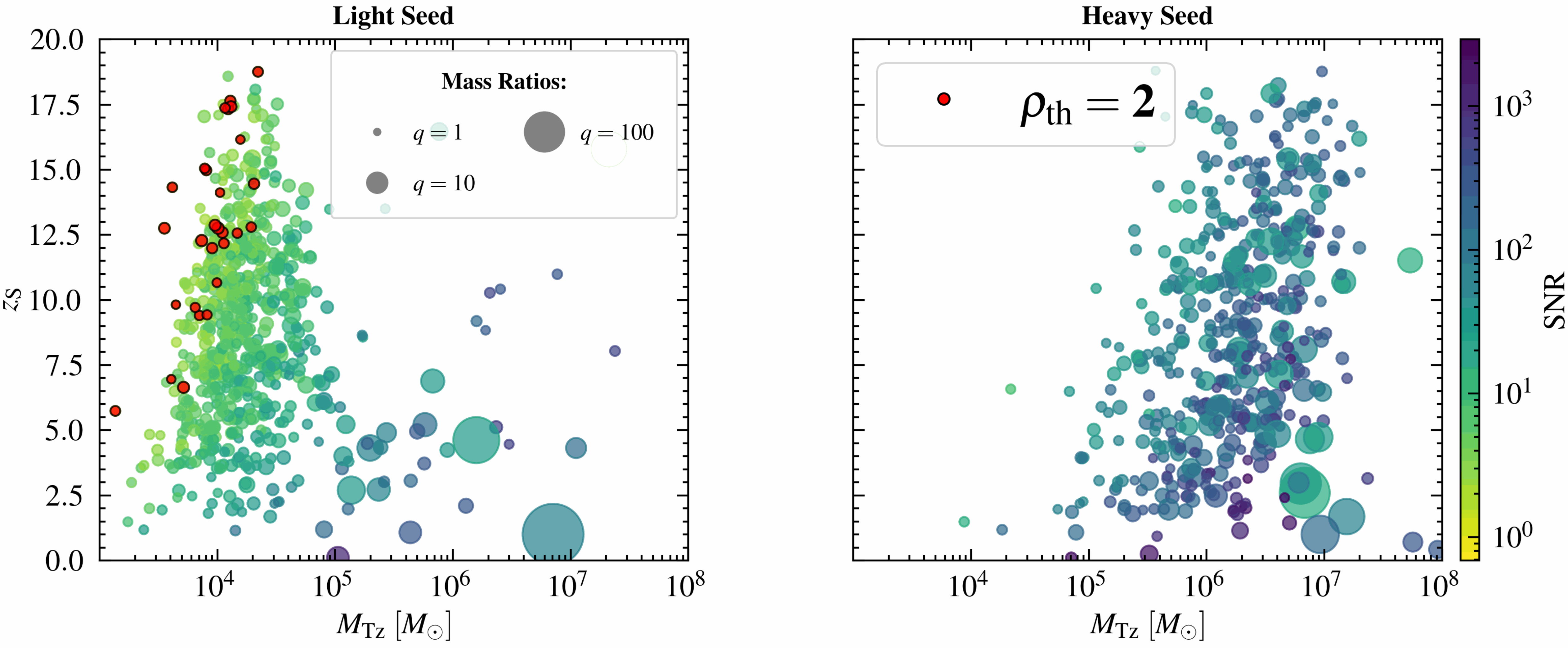

[Adopted from **Çalışkan**, et al. (2023) | Populations Based on Barausse, et al. (2023)]

LIMITATIONS

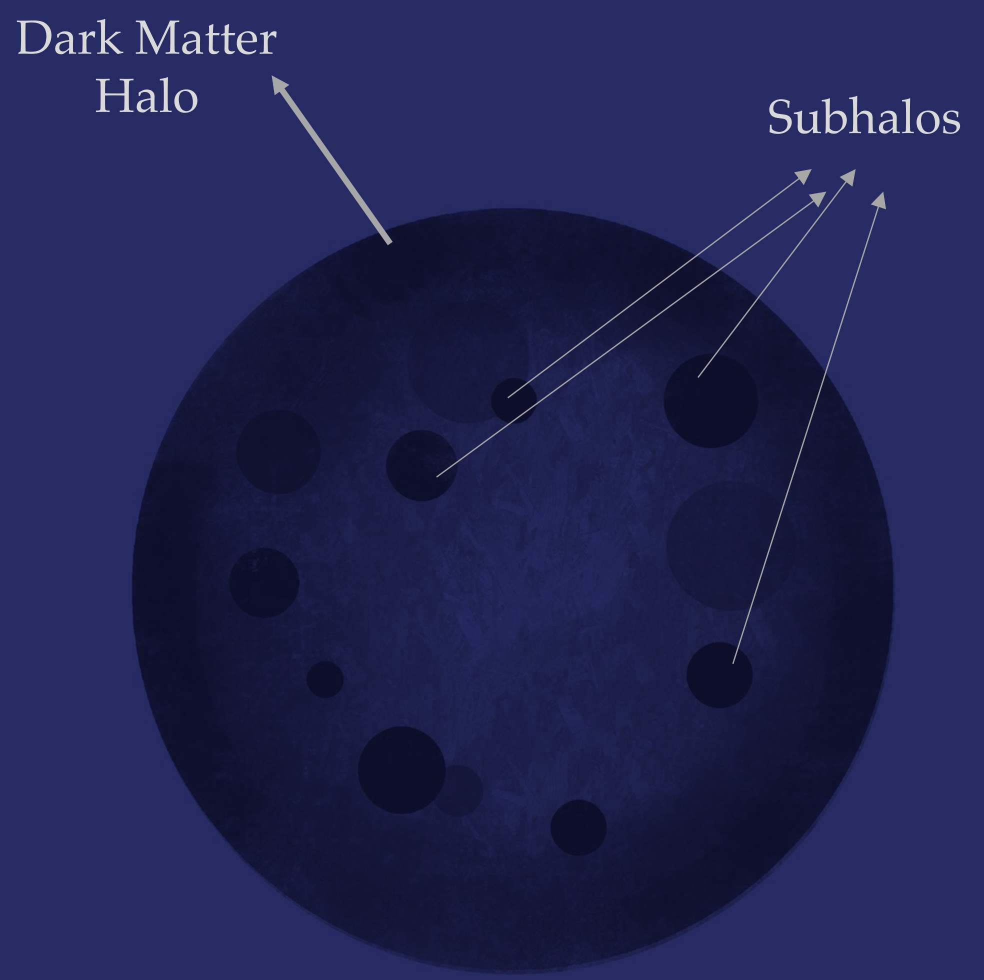

Illustration by Neha Anil Kumar

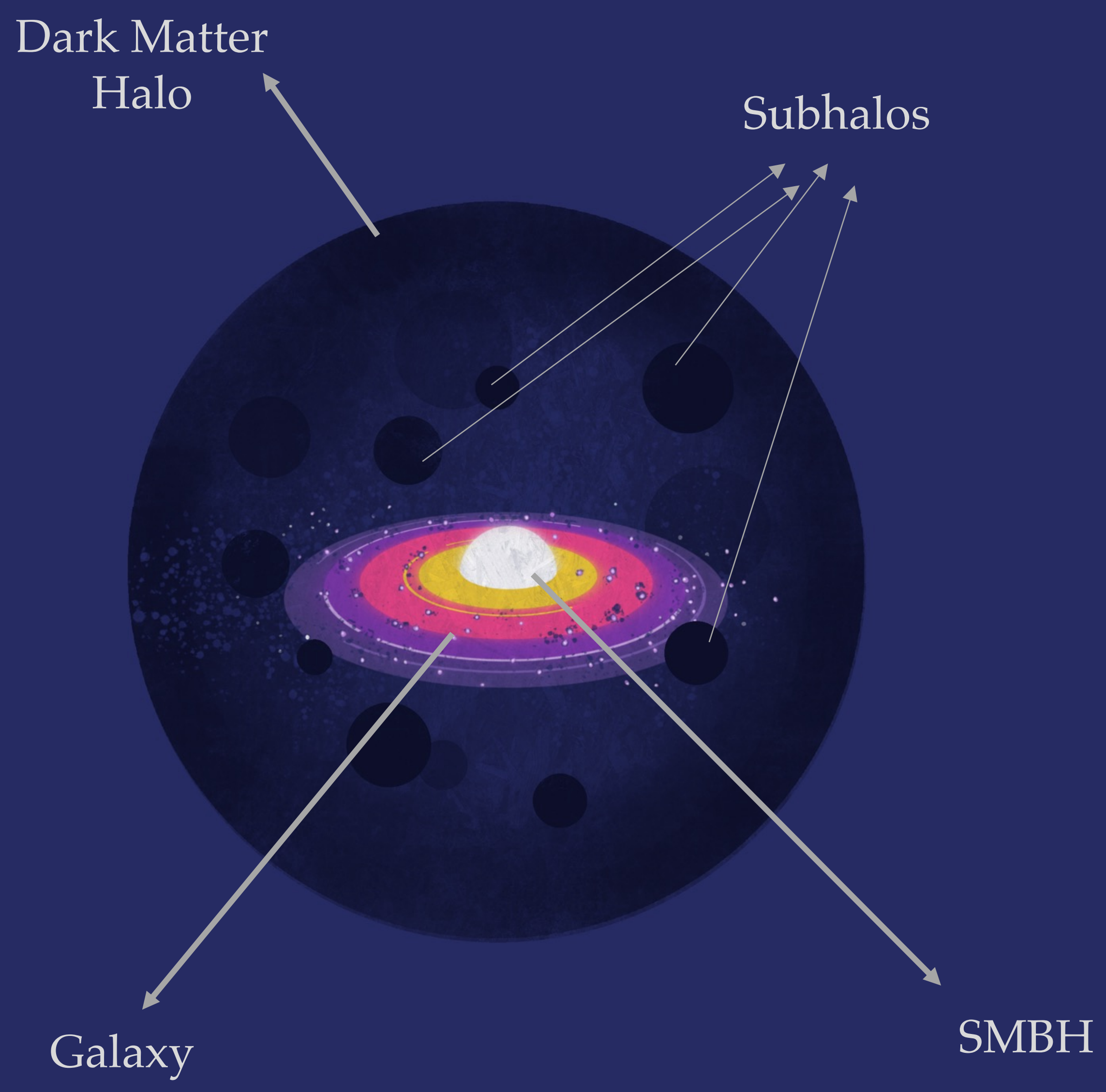

Illustration by Neha Anil Kumar

Diffractive Lensing of Gravitational Waves as a New Probe of Dark Matter[*]

Mesut Çalışkan[, α]

[1]*Johns Hopkins University*

BCCP Journal Club – 18 November 2025

[α] **caliskan@jhu.edu**

[*] arXiv: **2201.04619, 2206.02803, 2307.06990**

APPENDIX

Total Number of Binaries in the Population

Expected Number of Lensed Binaries with WO Effects (for Varying Detection Thresholds)

Resulting Lensing Rate

Source Population	Lens Population	N_{detect}	$N^{1\sigma}_{\text{lensed}}$	$N^{3\sigma}_{\text{lensed}}$	$N^{5\sigma}_{\text{lensed}}$	Lensing Rate $\{1\sigma, 3\sigma, 5\sigma\}$ [%]
Heavy Seed (No Delay)	PS	474	**7.96**	**4.13**	**3.24**	{1.68, 0.87, 0.68}
Heavy Seed (No Delay)	MVF	474	0.42	0.36	0.35	{0.09, 0.07, 0.07}
Heavy Seed (Delay)	PS	32	0.47	0.21	0.15	{1.47, 0.65, 0.47}
Heavy Seed (Delay)	MVF	32	0.01	0.009	0.008	{0.03, 0.03, 0.03}
Light Seed	PS	282	**1.51**	0.57	0.37	{0.53, 0.20, 0.13}
Light Seed	MVF	282	0.02	0.01	0.01	{0.007, 0.004, 0.004}

[4] **Çalışkan**, et al. (2023b)

Lensing Diffraction Integral

$$F(w, y)$$

for Point Mass and SIS Lenses

- $w = 8\pi M_{\rm Lz} f$
- $y :=$ Impact Parameter (Source Position)

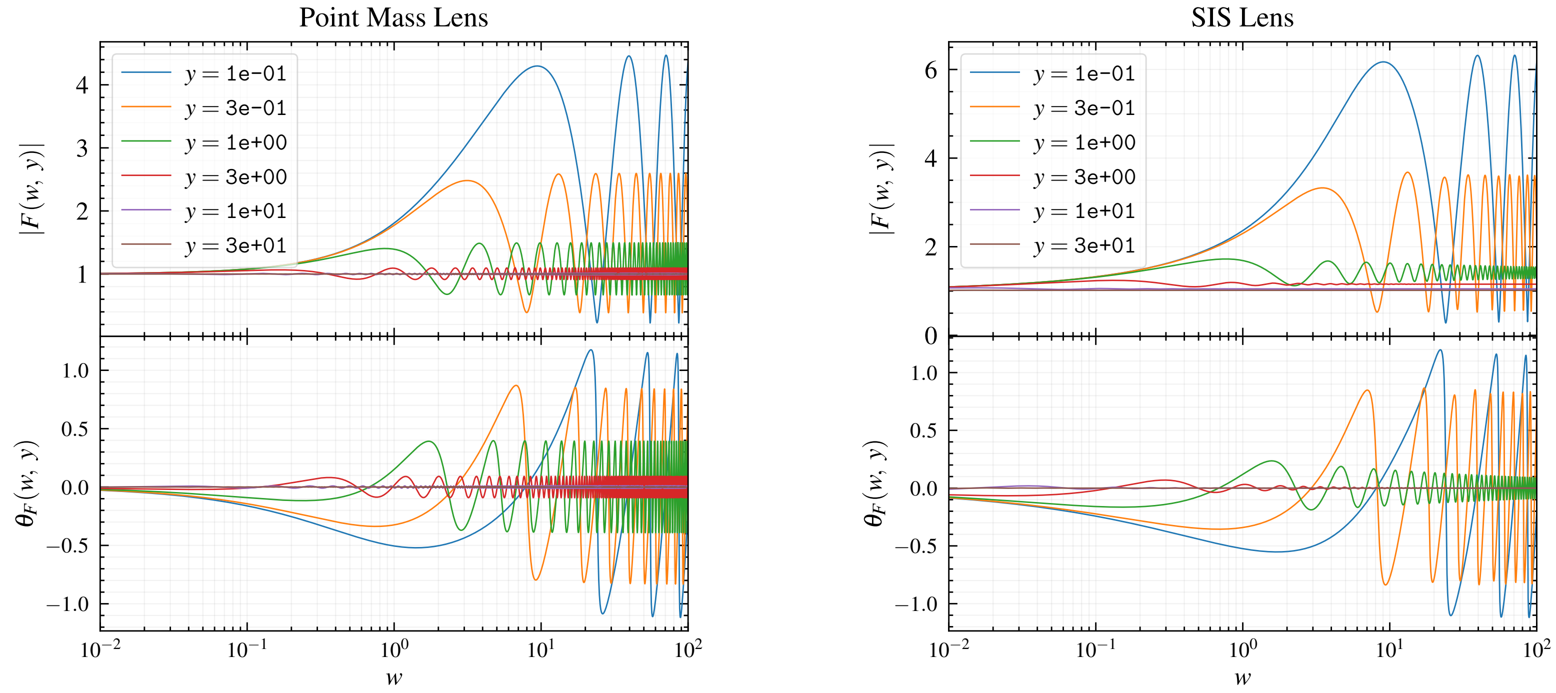

Lensed and Unlensed Waveforms

$$\tilde{h}^L(f; w, y) = F(w, y)\tilde{h}(f)$$

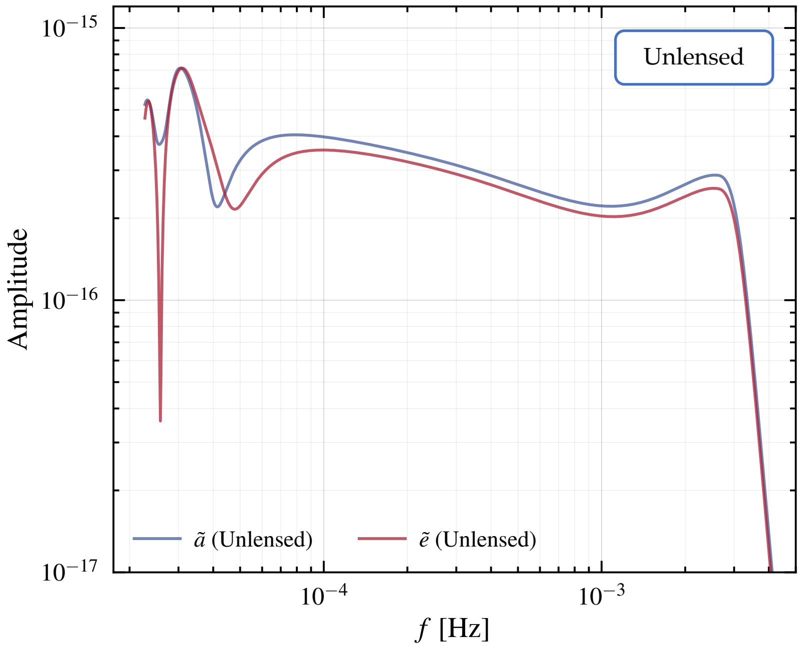

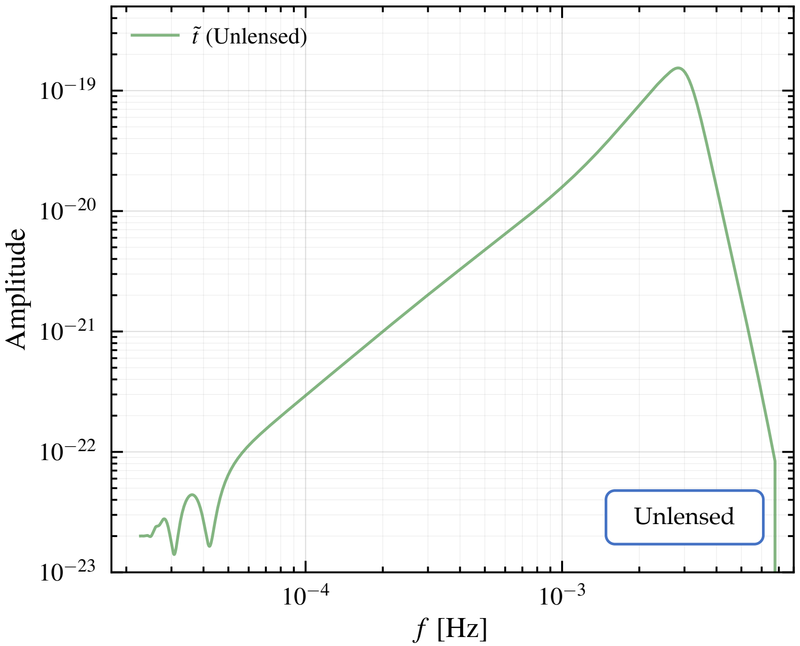

Lensing Diffraction Integral $F(w, y)$ for Point Mass and SIS Lenses

- $w = 8\pi M_{\mathrm{Lz}} f$
- $y :=$ Impact Parameter (Source Position)

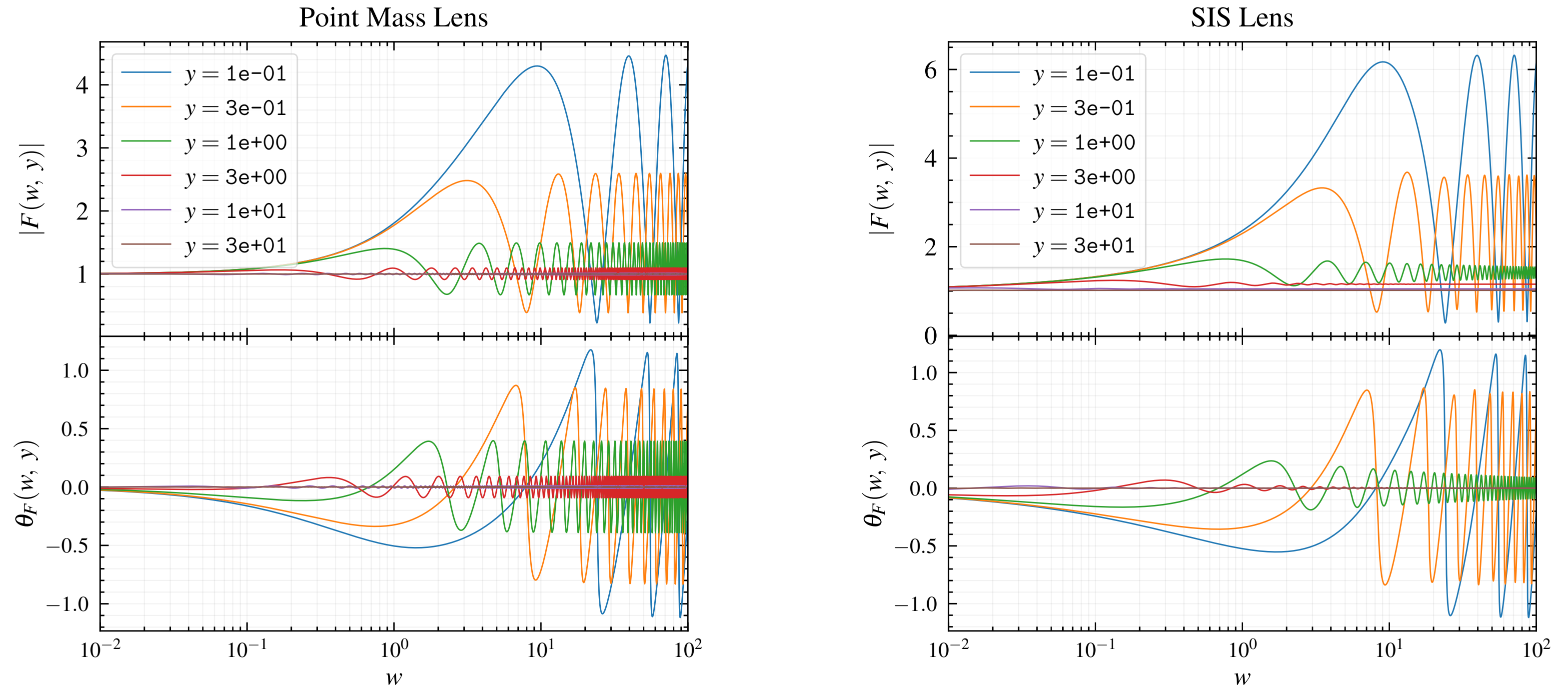

Lensed and Unlensed Waveforms

$$\tilde{h}^L(f; w, y) = F(w, y)\tilde{h}(f)$$

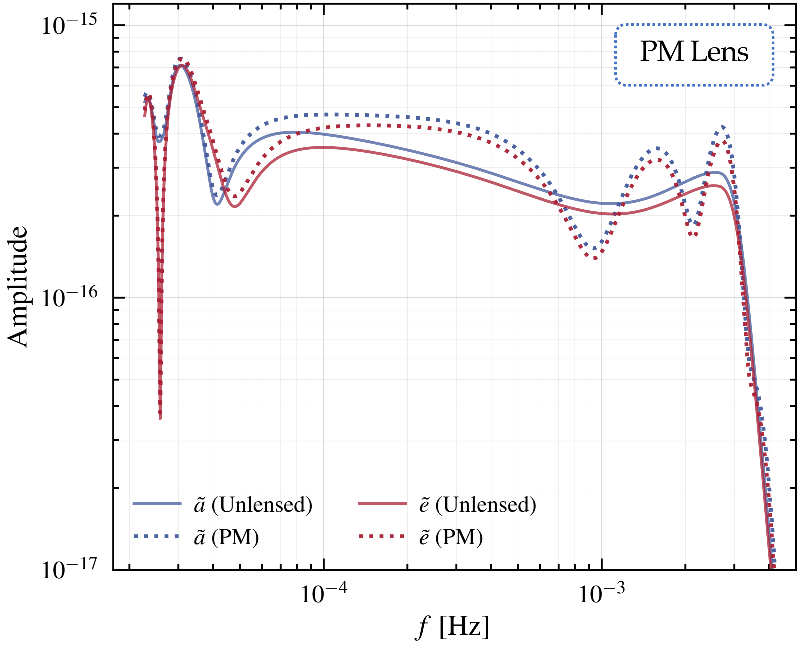

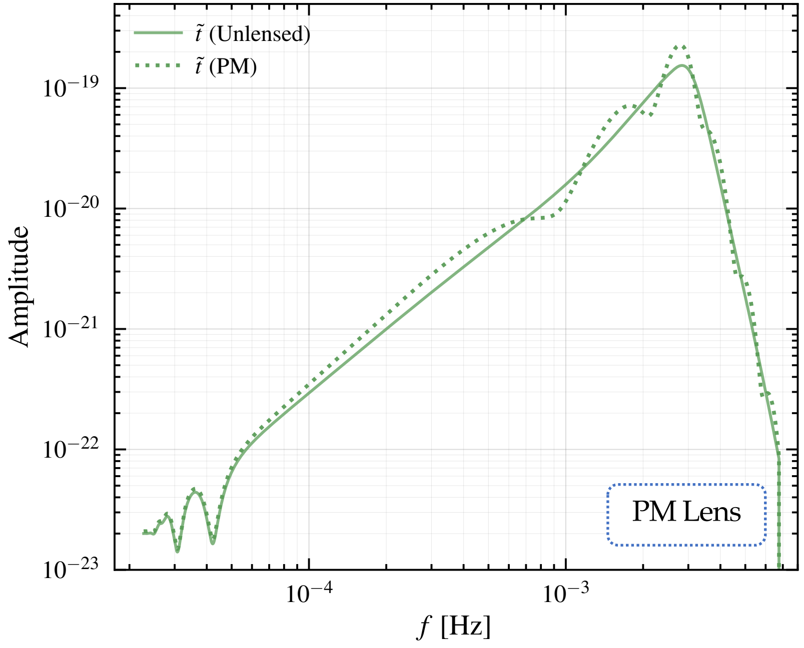

What Did We (the Field) Miss Before?

Inspiral-Only

- $M_{\mathrm{Tz}} = 2 \times 10^6\, M_\odot$
- $q = 1$
- $z_{\mathrm{S}} = 1$
- $\chi_1 = \chi_2 = 0$

- PM Lens
- $y = 0.1$

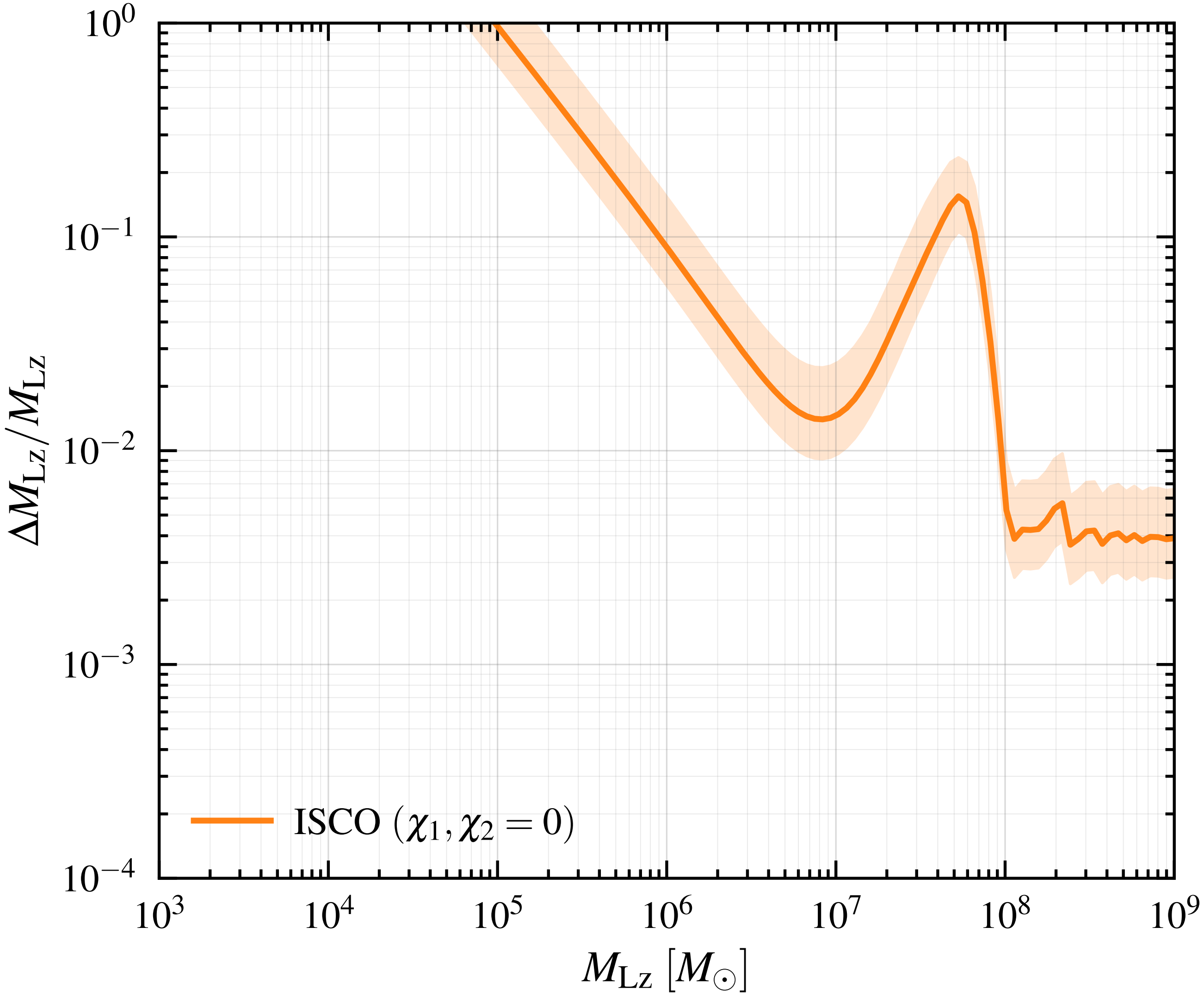

[3] **Çalışkan** et al. (2023a)

Merger!

- $M_{\mathrm{Tz}} = 2 \times 10^6\, M_\odot$
- $q = 1$
- $z_{\mathrm{S}} = 1$
- $\chi_1 = \chi_2 = 0$

- PM Lens
- $y = 0.1$

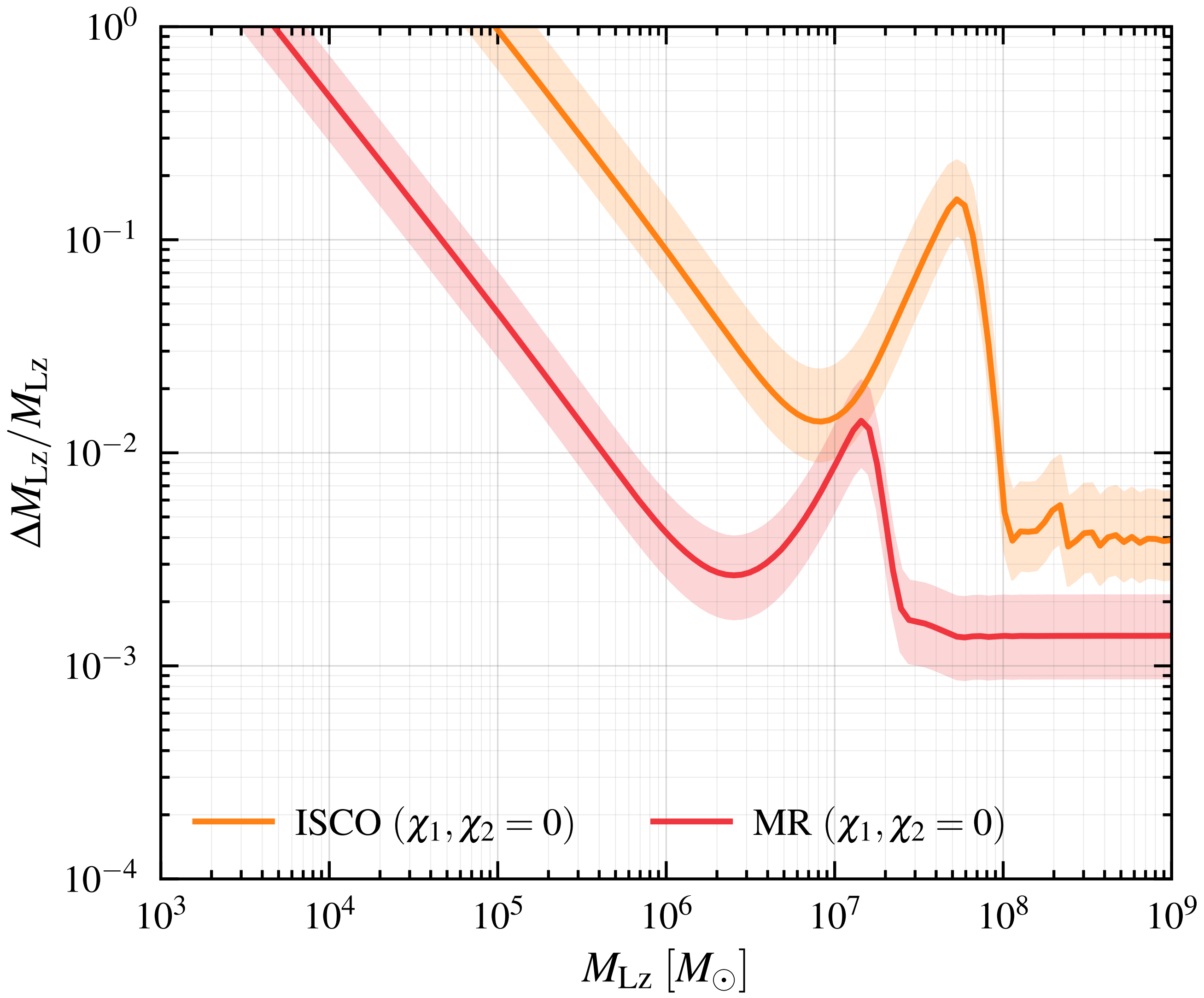

[3] **Çalışkan** et al. (2023a)

Why?

Because the SNR is higher?

- $M_{\mathrm{Tz}} = 2 \times 10^6\, M_\odot$
- $q = 1$
- $z_{\mathrm{S}} = 1$
- $\chi_1 = \chi_2 = 0$

- PM Lens
- $y = 0.1$

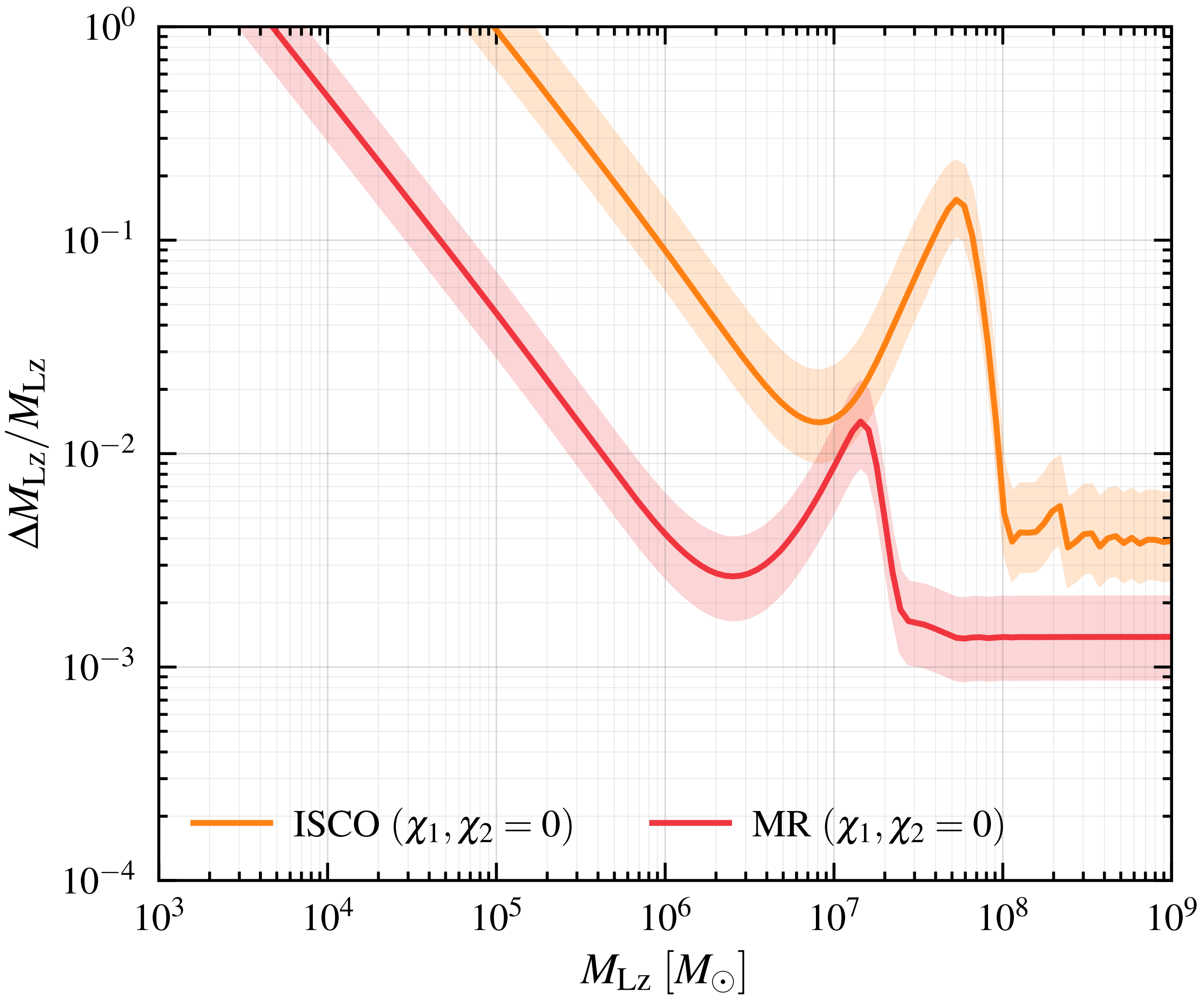

[3] **Çalışkan** et al. (2023a)

Higher-Order Modes?

- $M_{\mathrm{Tz}} = 2 \times 10^6\, M_\odot$
- $q = 1$
- $z_{\mathrm{S}} = 1$
- $\chi_1 = \chi_2 = 0$

- PM Lens
- $y = 0.1$

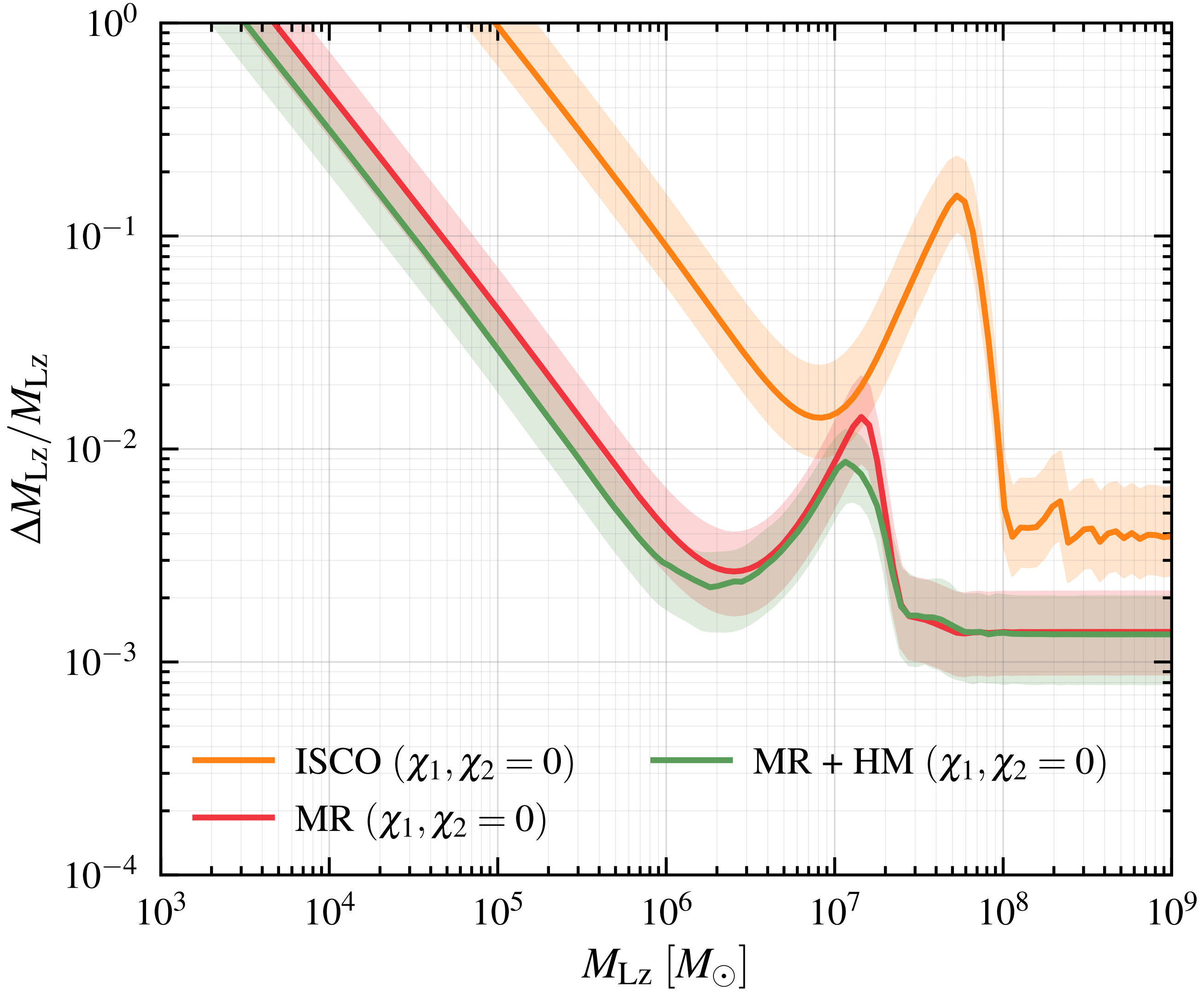

[3] **Çalışkan** et al. (2023a)

We Need Faster Solutions

Singular Isothermal Sphere (SIS) Lens

- $$F(\underbrace{w}_{w=8\pi M_{\mathrm{Lz}} f}, y) = \frac{w}{i} \exp\left\{ iw \left[\frac{y^2}{2} + \underbrace{\phi(y)}_{y+\frac{1}{2}} \right] \right\} \int_0^\infty x \mathrm{d}x \, \exp\left\{ iw \left[\frac{x^2}{2} - \underbrace{\psi(x)}_{x} \right] \right\} J_0(wxy)$$

   - Taylor expansion of the exponential factor $\exp[-iw\psi(x)]$

   - $$I_n(w,y) \equiv \int_0^\infty x^n e^{iwx^2/2} J_0(wxy)\, x\mathrm{d}x = \frac{1}{2}\left(\frac{2i}{w}\right)^N \Gamma(N)\, {}_1F_1\left(\underbrace{N}_{N\equiv(n+2)/2}, 1; -i\frac{wy^2}{2}\right)$$

   - $$\Psi(w,x) \equiv e^{-iw\psi(x)} = \sum_{n=0}^{\infty} \Psi_n(w) x^n$$

$$\Psi_n(w) = (-iw)^n / n!$$

[3] **Çalışkan** et al. (2023a)

[14] Matsunaga and Yamamoto (2006)

PM Lens

SIS Lens

- $$F(w,y) = \exp\left\{\frac{\pi w}{4} + i\frac{w}{2}\left[\ln\frac{w}{2} - 2\phi(y)\right]\right\}\Gamma\left(1-\frac{w}{2}i\right){}_1F_1\left(\frac{w}{2}i, 1; \frac{wy^2}{2}i\right)$$

- $$F(w,y) = \frac{w}{i}\exp\left\{iw\left[\frac{y^2}{2}+\phi(y)\right]\right\}\sum_{n=0}^{\infty}\Psi_n(w)I_n(w,y)$$

- $$\Gamma(z) = \left\{z\, e^{cz}\prod_{r=1}^{\infty}\left[\left(1+\frac{z}{r}\right)e^{-z/r}\right]\right\}^{-1}$$
- $$\Gamma'(z) = \Gamma(z)\ \Psi(z)$$

$$\left.\right\} \frac{\partial\Gamma\left(1-\frac{w}{2}i\right)}{\partial w} = -\frac{1}{2}i\ \Gamma\left(1-\frac{w}{2}i\right)\ \Psi\left(1-\frac{w}{2}i\right)$$

- $${}_1F_1(a,b;z) = 1 + \frac{a}{b}\frac{z}{1!} + \frac{a(a+1)}{b(b+1)}\frac{z^2}{2!} + \ldots$$

$$\left.\right\} \frac{\partial\, {}_1F_1(a,b;z)}{\partial z} = \frac{a}{b}\ {}_1F_1(a+1,b+1;z)$$

$$\frac{\partial\, {}_1F_1(a,b;z)}{\partial a} = \sum_{k=0}^{\infty}\frac{(a)_k\Psi(a+k)z^k}{k!(b)_k} - \Psi(a){}_1F_1(a,b;z)$$

- $$\begin{aligned}\frac{\partial\, {}_1F_1(a,b;z)}{\partial w} &= \frac{\partial\, {}_1F_1(a,b;z)}{\partial a}\cdot\frac{\partial a}{\partial w} + \frac{\partial\, {}_1F_1(a,b;z)}{\partial z}\cdot\frac{\partial z}{\partial w}\\ &= \frac{i}{2}\cdot\frac{\partial\, {}_1F_1(a,b;z)}{\partial a} + \frac{y^2}{2}i\cdot\frac{\partial\, {}_1F_1(a,b;z)}{\partial z}\\ &= \frac{i}{2}\sum_{k=0}^{\infty}\frac{(i\frac{w}{2})_k\Psi(i\frac{w}{2}+k)z^k}{k!(1)_k} - \Psi\left(i\frac{w}{2}\right)\ {}_1F_1\left(i\frac{w}{2},1;i\frac{wy^2}{2}\right) - \frac{wy^2}{4}\ {}_1F_1\left(i\frac{w}{2}+1,2;i\frac{wy^2}{2}\right)\end{aligned}$$

- $$\frac{\partial\, {}_1F_1(a,b;z)}{\partial y} = -\frac{w^2y}{2}\ {}_1F_1\left(\frac{w}{2}i+1,2;\frac{wy^2}{2}i\right)$$

- $$\frac{\partial\Psi_n(w)}{\partial w} = \frac{(-i)^n}{(n-1)!}w^{n-1}$$

- $$\frac{\partial I_n(w,y)}{\partial w} = \frac{N}{2}\left(\frac{2i}{w}\right)^N\Gamma(N)\left[\left(-i\frac{y^2}{2}\right)\ {}_1F_1\left(N+1,2;-i\frac{wy^2}{2}\right) - \frac{1}{w}\ {}_1F_1\left(N,1;-i\frac{wy^2}{2}\right)\right]$$

- $$\frac{\partial I_n(w,y)}{\partial y} = -iN\frac{wy}{2}\left(\frac{2i}{w}\right)^N\Gamma(N)\ {}_1F_1\left(N+1,2;-i\frac{wy^2}{2}\right)$$

- $$\frac{\partial F(w,y)}{\partial w} = \frac{\partial E(w,y)}{\partial w}\sum_{n=0}^{\infty}\Psi_n(w)I_n(w,y) + E(w,y)\sum_{n=0}^{\infty}\left[\frac{\partial\Psi_n(w)}{\partial w}I_n(w,y) + \Psi_n(w)\frac{\partial I_n(w,y)}{\partial w}\right]$$

- $$\frac{\partial F(w,y)}{\partial y} = \frac{\partial E(w,y)}{\partial y}\sum_{n=0}^{\infty}\Psi_n(w)I_n(w,y) + E(w,y)\sum_{n=0}^{\infty}\Psi_n(w)\frac{\partial I_n(w,y)}{\partial y}$$

[3] **Çalışkan** et al. (2023a)

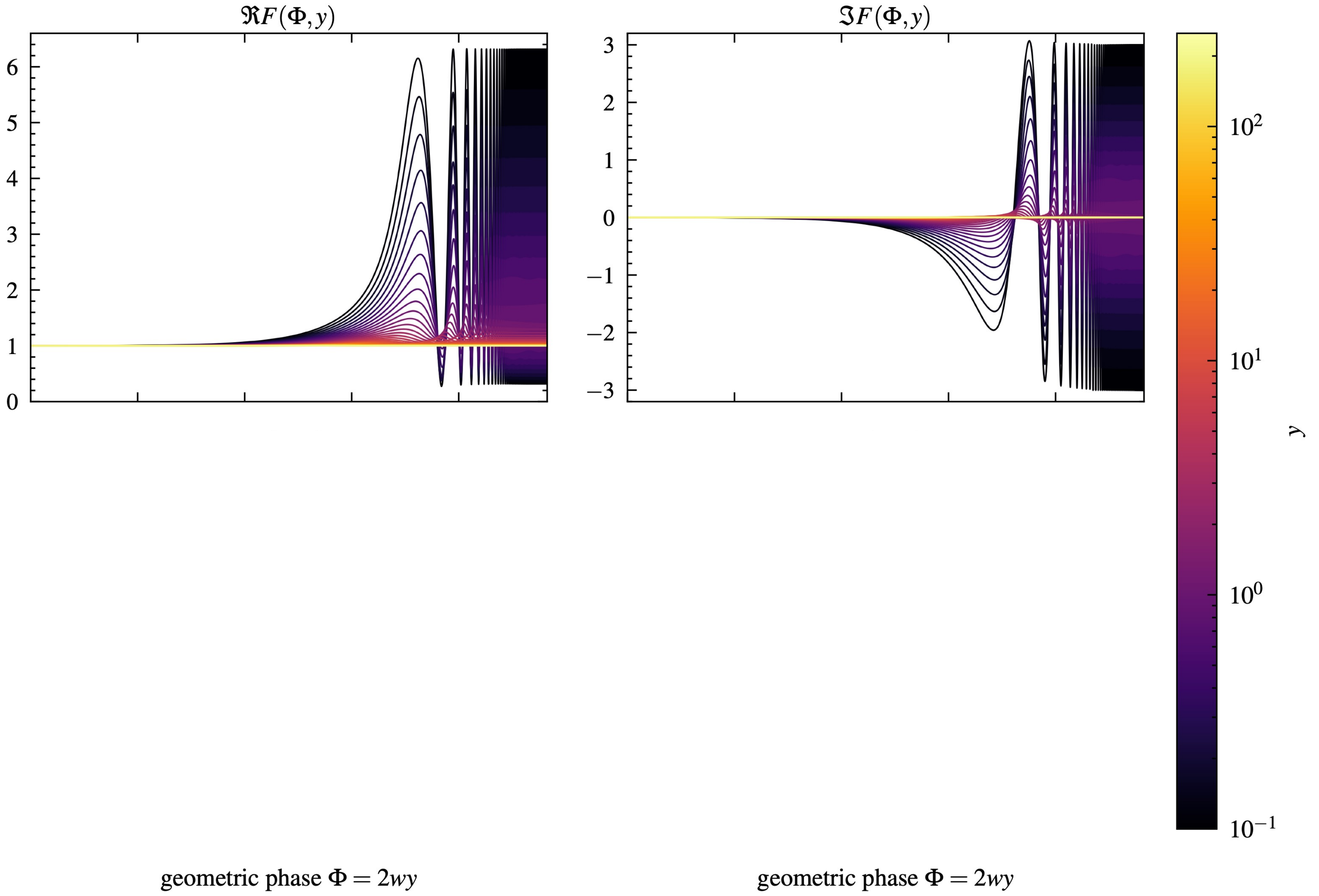

[4] **Çalışkan**, Anil Kumar, et al. (2023b)

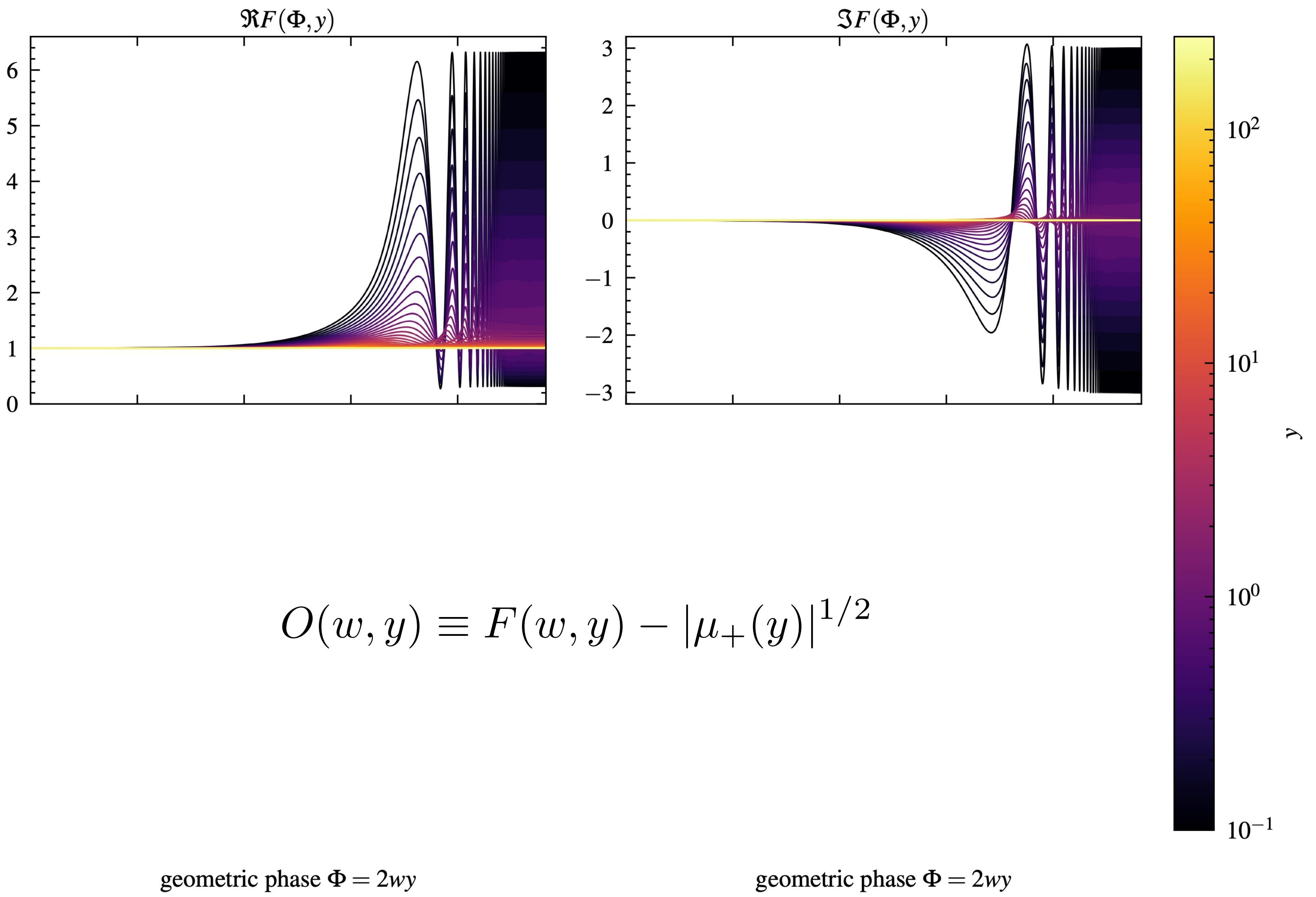

$$O(w,y) \equiv F(w,y) - |\mu_+(y)|^{1/2}$$

[4] **Çalışkan**, Anil Kumar, et al. (2023b)

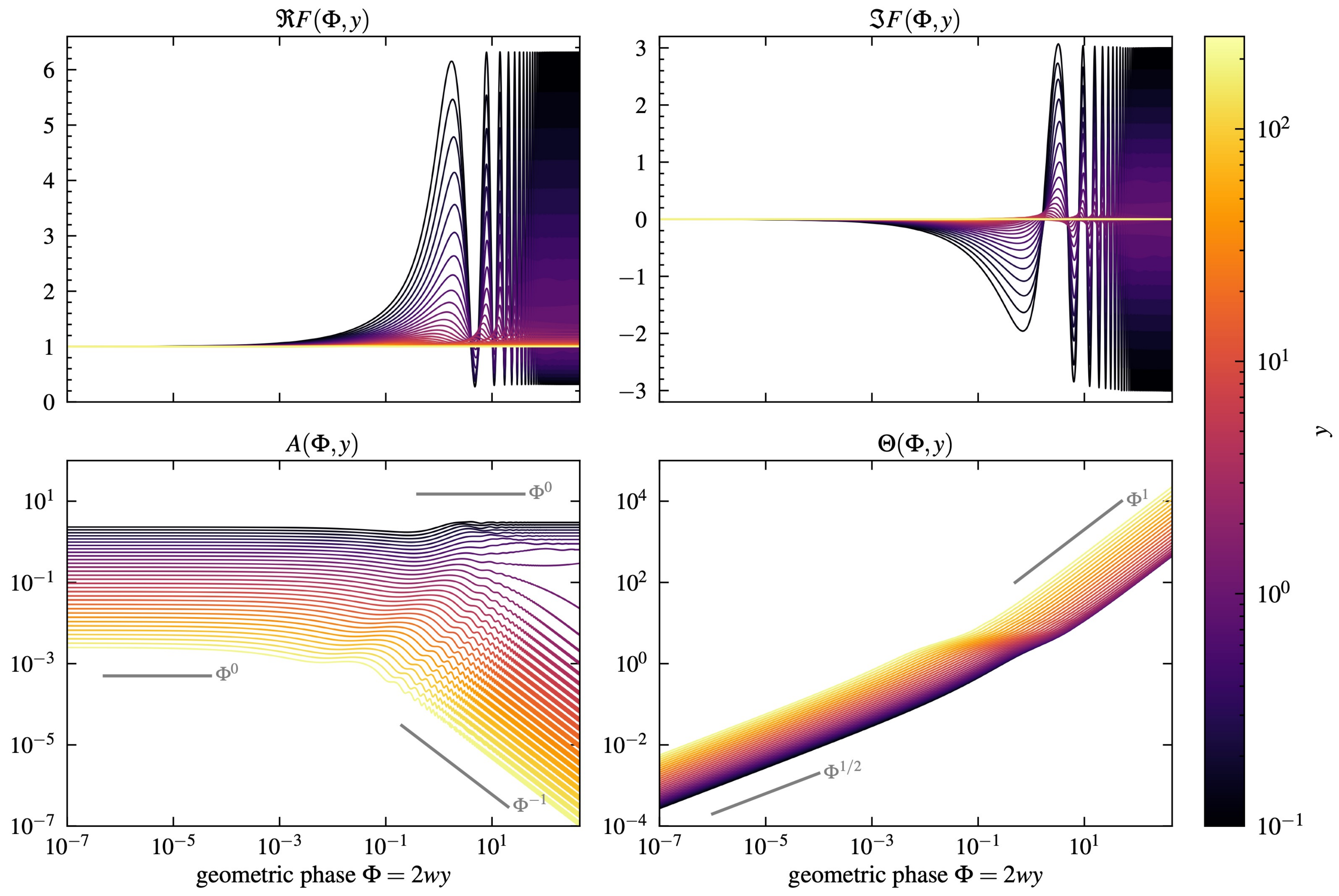

[4] **Çalışkan**, Anil Kumar, et al. (2023b)

Detectable (Sub)halo Mass Range

Detectable Halo Mass Range

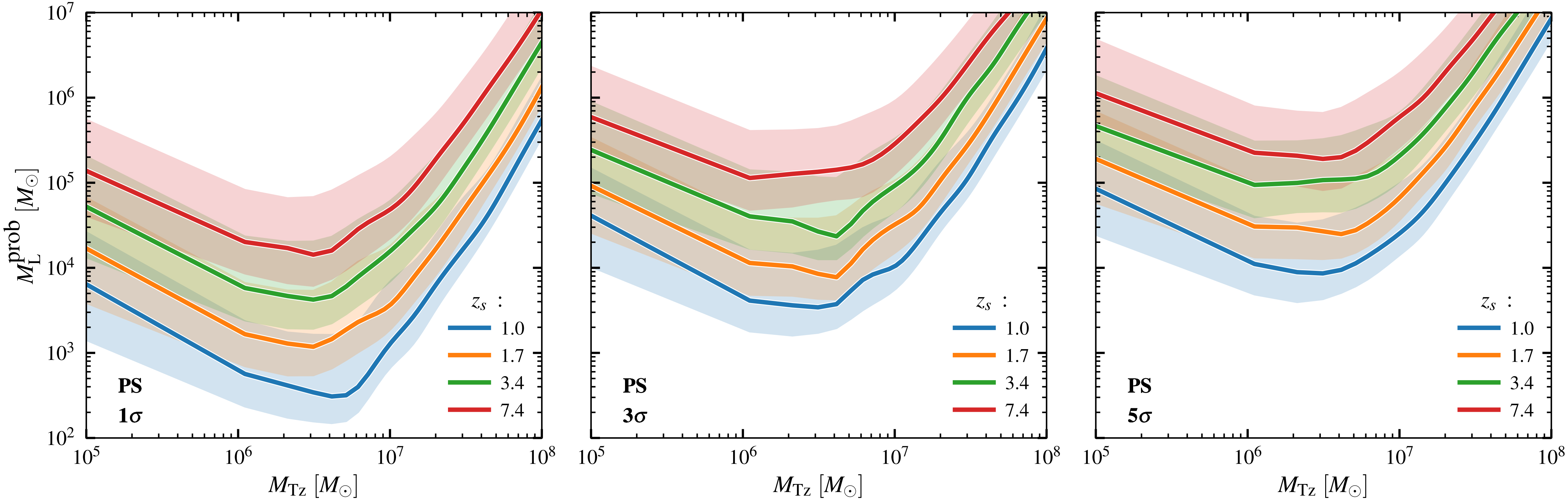

[4] **Çalışkan**, Anil Kumar, et al. (2023b)

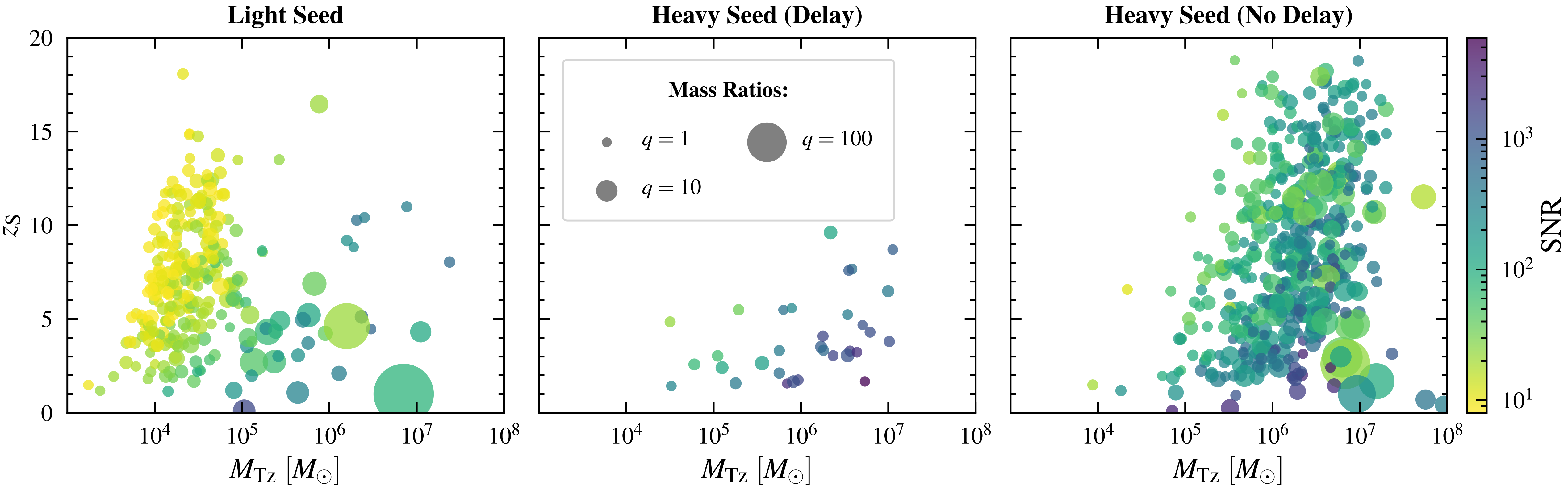

[4] **Çalışkan**, Anil Kumar, et al. (2023b)
[11] Barausse (2012)
[12] Klein, Barausse, et al. (2016)

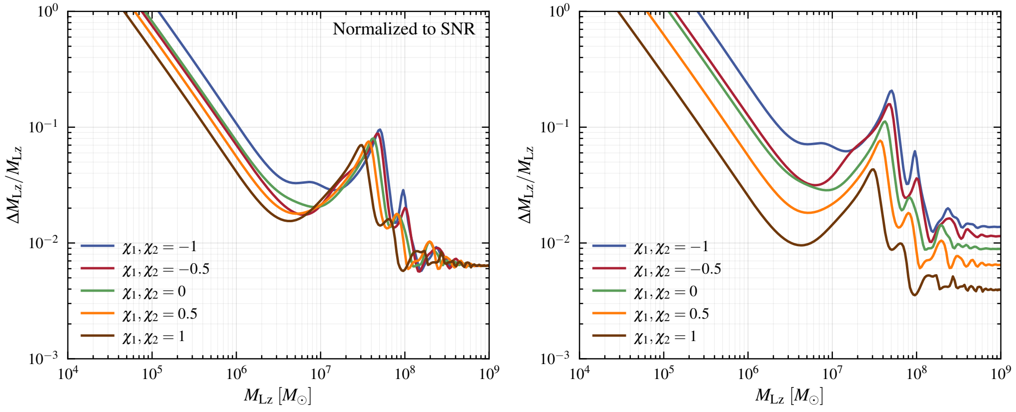

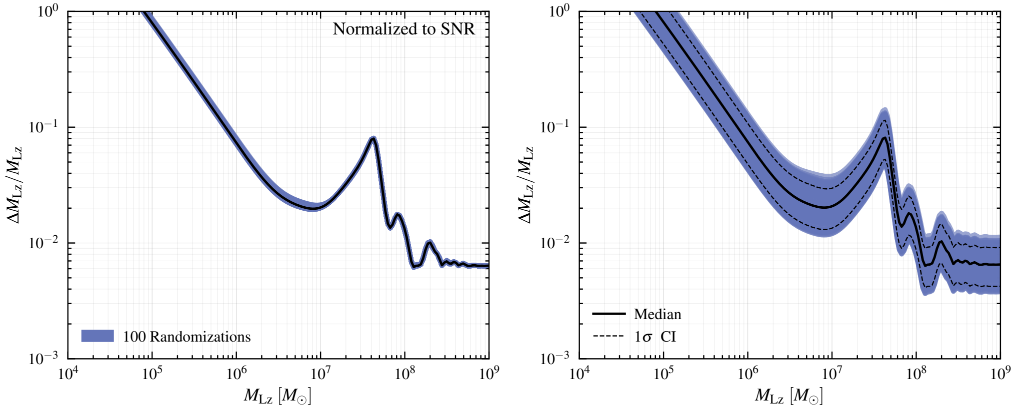

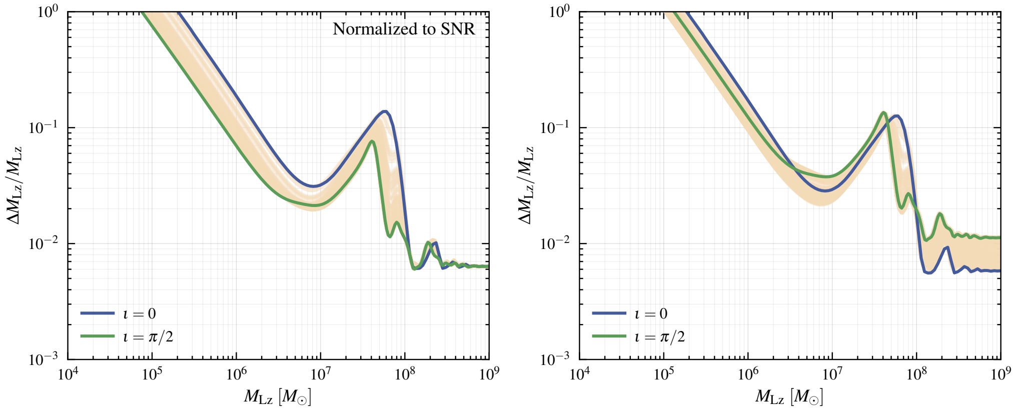

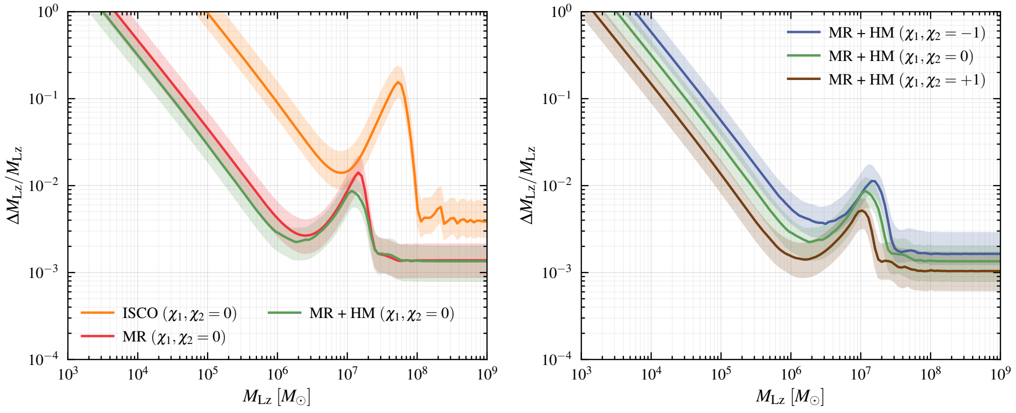

[4] **Çalışkan** et al. (2023a)

Information Matrix Formalism

- $\boldsymbol{\theta}^{\mathrm{S}} \equiv \{\mathcal{M}_{\mathrm{z}},\ q,\ d_l,\ t_{\mathrm{c}},\ \iota,\ \phi_{\mathrm{c}},\ \lambda,\ \beta,\ \psi,\ \chi_{\mathrm{m}},\ \chi_{\mathrm{p}}\}$

  Detector-Frame Chirp Mass
  Mass Ratio
  Luminosity Distance
  Time of Coalescence
  Inclination
  Coalescence Phase
  Right Ascension
  Declination
  Polarization Angle
  2 Aligned-Spin Parameters

- $\boldsymbol{\theta}^{\mathrm{L}} \equiv \{M_{\mathrm{Lz}},\ y\}$

  Redshifted Lens Mass
  Impact Parameter

$$\boldsymbol{\theta} \equiv \{\boldsymbol{\theta}^{\mathrm{S}}, \boldsymbol{\theta}^{\mathrm{L}}\}$$

13×13 Variance-Covariance Matrix

- Phenomenological Gravitational Waveform Models such as `IMRPhenomD` [3, 4] and `IMPRhenomHM` [5]

[3] Husa et al. (2016)
[4] Khan et al. (2016)
[5] London et al. (2018)

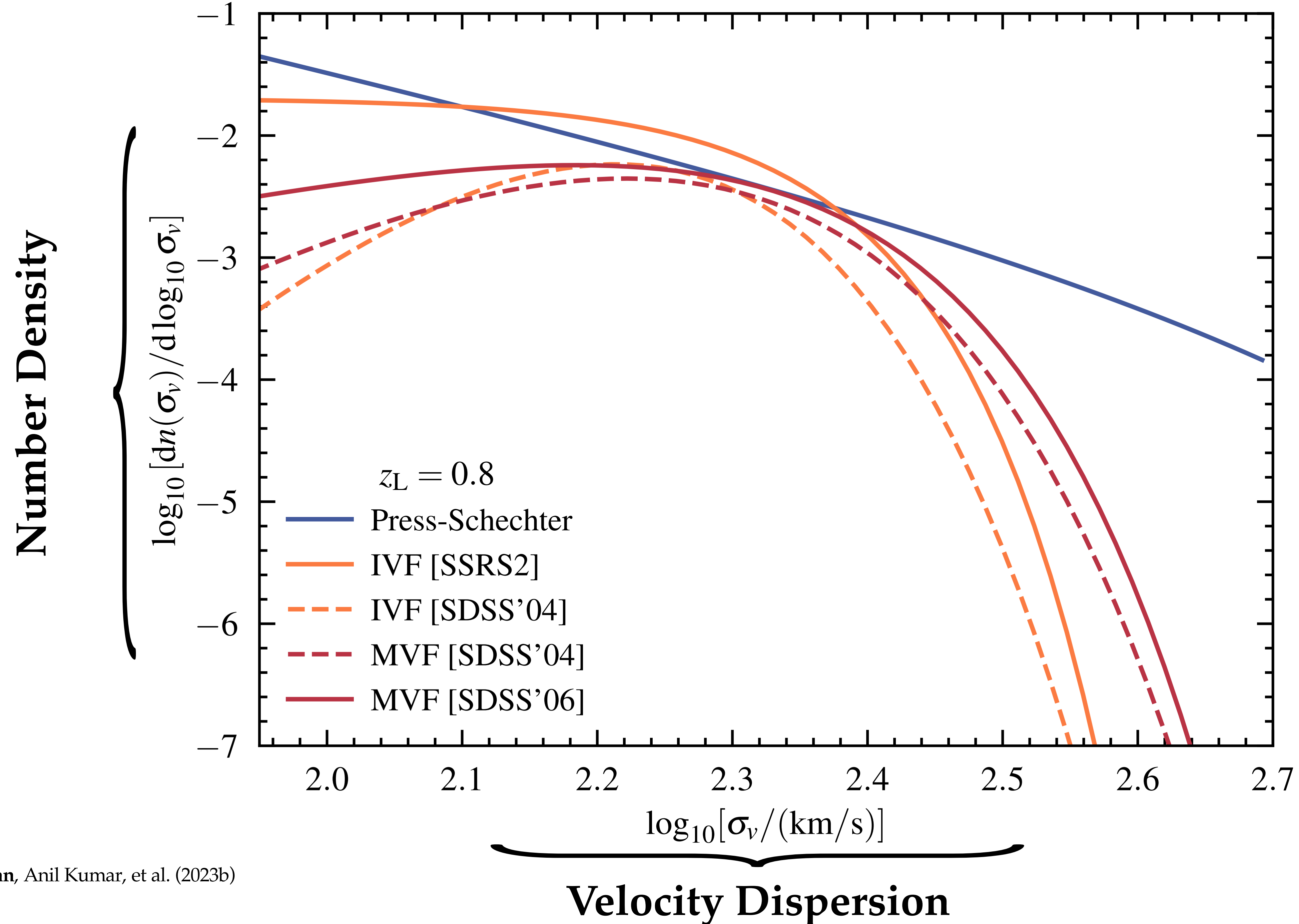

[5] **Çalışkan**, Anil Kumar, et al. (2023b)

Singular Isothermal Sphere with an Outside Boundary

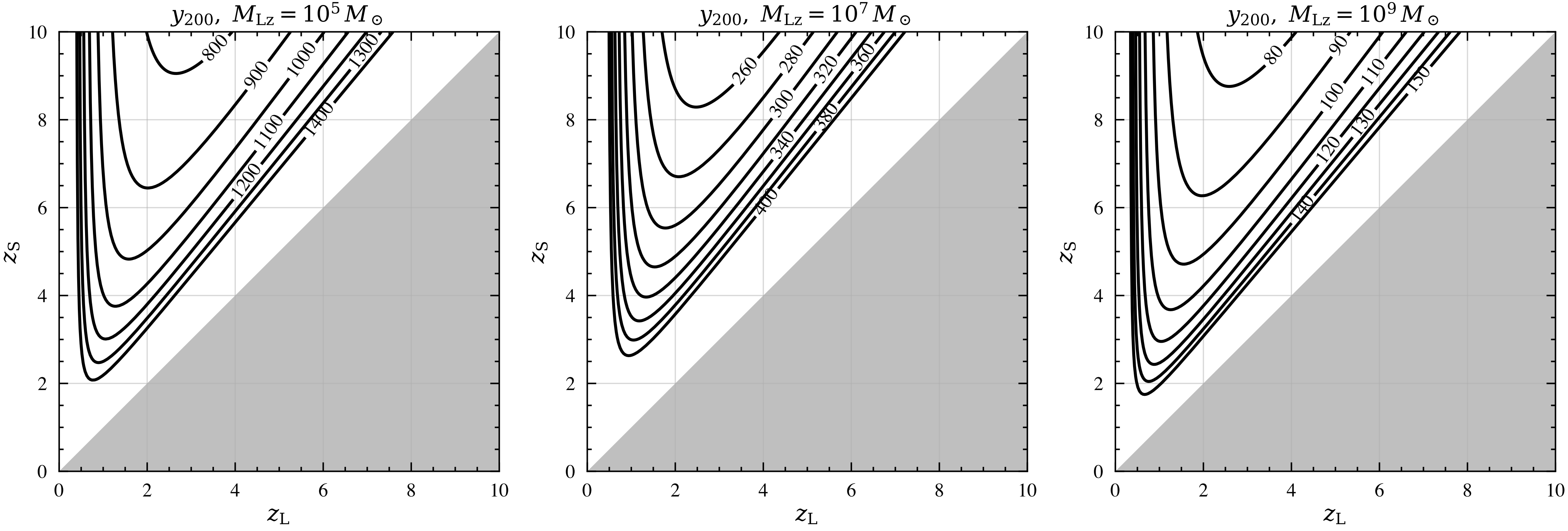

Thus, the truncation of the SIS profile is irrelevant in the range of potentially detectable values of y.